

https://dspace.org/

Mapping SARS-CoV-2 spike determinants of escape from antibodies

Musvosvi, Bliss

2022
https://hdl.handle.net/10539/34270

Downloaded from a DSpace repository. https://dspace.org/

UNIVERSITY OF WITWATERSRAND

FACULTY OF HEALTH SCIENCES

SCHOOL OF PATHOLOGY

Mapping SARS-CoV-2 spike determinants of escape from antibodies

Student Name: Bliss Musvosvi

Student number: 2373493

Program: MSc (Med) Vaccinology

Supervisors:

Dr. Thandeka Moyo-Gwete

Prof Penny Moore

Dr. Jinal Bhiman

Dr. Clare Cutland

Declaration

I, Bliss Musvosvi, declare that this research report is my own work. It is being submitted for the degree of Masters of Science (Med) in the field of vaccinology at the University of the Witwatersrand, Johannesburg, South Africa. It has not been submitted previously for any degree or examination at this or any other university.

Signature: 

Date: 1 June 2022

Place: 70 Gamtoosrivier drive, Norkem Park, Kempton Park, 1628, South Africa,

Dedication

I dedicate this work to my mother, Tembekile Musvosvi.

Acknowledgements

I acknowledge my supervisors, Dr. Thandeka Moyo-Gwete, Dr. Jinal Bhiman, Professor Penny Moore and Dr. Clare Cutland for their continued support and training during this project. Special acknowledgement to Dr.Thandeka Moyo-Gwete for her day-to-day hands on training and guidance. I would like to acknowledge and thank the African Leadership in Vaccine Expertise (ALIVE) consortium for their technical and financial support and the opportunities that they have provided me throughout my masters trainining. I would further like to acknowledge the National institute for communicable diseases - Centre for HIV and STI and the lab members for their facilities and technical expertise. I acknowledge my family, friends and partner for their continued love and encouragement throughout my study and research. Lastly, I would like to thank God almighty for sustaining me through this course.

Abstract

Severe acute respiratory syndrome coronavirus 2 (SARS-CoV-2) causes COVID-19 disease and has resulted in a global pandemic that has subsequently led to the search for effective interventions. The spike protein plays a crucial role in viral entry into host cells and it has many epitopes that are recognized by neutralizing antibodies making it a target of vaccines. Monitoring and evaluation of the evolution of SARS-CoV-2 is essential as emerging variants may alter the effectiveness of natural and vaccine induced immune responses. The aim of this study was to probe the effect of emerging variants detected in South Africa on neutralization by SARS-CoV-2 directed antibodies in convalescent plasma. Four SARS-CoV-2 sublineages circulating in South Africa during December 2020 were identified in a parent study and characterized in this study. Protein analysis software tools were used to visualize changes in structural interactions between the spike and the angiotensin-converting enzyme 2 (ACE2) receptor and monoclonal antibodies after *in silico* mutation of relevant residues in the protein structure. Site-directed mutagenesis was used to introduce sublineage mutations into the wild type spike gene sequence. Wild type and mutated SARS-CoV-2 spike trimer proteins were generated and characterized by mammalian cell expression, chromatography-based protein purification and Sodium dodecyl-sulfate polyacrylamide gel electrophoresis (SDS-PAGE). The effect of mutations on the binding of SARS-CoV-2 directed antibodies was assessed by enzyme-linked immunoassay (ELISA). Wild type and mutated SARS-CoV-2 spike-pseudotyped viruses were also generated. The impact of viral mutations on the neutralization capacity of the antibodies present in convalescent plasma elicited by the ancestral strain was assessed. The results of this study revealed that convalescent plasma had reduced binding to two local sub-lineage viruses when compared to the wild type virus. The change in binding may have resulted from mutations that cause the loss of epitope recognition. No significant changes were observed in the neutralization sensitivity when the wild type was compared to sub-lineage pseudoviruses, however, significant differences in neutralization sensitivity were observed when sublineages were compared with other sub-lineages characterized in this study. This study supports current literature on the need for robust genomic surveillance and immune characterization of emerging variants and related sub-lineages.

TABLE OF CONTENTS

Declaration 2
Dedication 3
Acknowledgements 4
Abstract 5
CHAPTER ONE: LITERATURE REVIEW 10
1.1 The SARS-CoV-2 Pandemic 10
1.2 SARS-CoV-2 genome and spike glycoprotein structure 10
1.3 Humoral immune response to SARS-CoV-2 11
1.3.1 Neutralizing antibodies against the SARS-CoV-2 spike glycoprotein 12
1.4 SARS-CoV-2 spike evolution and the emergence of VOC/VOIs 14
1.5 SARS-CoV-2 vaccine efficacy against VOCs/VOIs 19
1.6 Study Aims and Objectives 22
CHAPTER TWO: METHODS 23
2.1 Cohort description 23
2.2 Ethical Approval 23
2.3 Identification of sub-lineages 24
2.3 Protein Structural Analysis 24
2.4 Site Directed Mutagenesis 24
2.5 XL-10 Gold Ultracompetent *E. Coli* Cell Transformation 25
2.6 DNA Extraction 25
2.7 DNA Sequencing 26
2.8 Maintenance of 293F, 293T, 293T/ACE2 cell lines 26
2.9 SARS-CoV-2 trimer expression, purification and size exclusion chromatography (SEC) 27
2.11 Sodium dodecyl sulphate–polyacrylamide gel electrophoresis 28
2.12 Enzyme Linked Immunosorbent Assay (ELISA) 28
2.13 Pseudovirus production 28
2.14 Neutralization assay 29
CHAPTER THREE: RESULTS 30
3.1 Sub-lineage mutations identified from SARS-CoV-2 infected individuals 30
3.2 Protein Structural Analysis 32
3.3 SARS-CoV-2 spike protein expression and purification 36
3.4 Change in binding between WT and Sub-lineage spike proteins 37
3.5 Neutralization Data 40

CHAPTER FOUR: DISCUSSION.....44
CONCLUSION 47
REFERENCES.....49

LIST OF FIGURES

CHAPTER ONE

Figure 1.1: Epidemiological Waves of SARS-CoV-2 in South Africa…….....10
Figure 1.2: Structure of the SARS-CoV-2 spike glycoprotein……11
Figure 1.3: Classification of antibodies based on location of epitope on spike glycoprotein……..……..13
Figure 1.4: SARS-CoV-2 Structure of the spike protomer showing the NTD…….14
Figure 1.5: Mutations affecting antibody classes……19

CHAPTER THREE

Figure 3.1: Schematic representation of the mutations in each sub-lineage and Nextclade sequence lineage assignment……..31
Figure 3.2: Percentage of GISAID sequences with mutations of interest…….....32
Figure 3.3: Change in protein interactions due to mutations in the spike glycoprotein……34
Figure 3.4: Change in protein interactions due to mutations in the spike glycoprotein……35
Figure 3.5: Size exclusion chromatograph profiles for purification of sub-lineage 1 – 4 proteins and Reducing and Non-reducing SDS PAGE confirm size of spike protein trimer……36
Figure 3.6: ELISA titration graphs for SARS-CoV-2 spike proteins……..….37
Figure 3.7: The change in binding between wild type and sub-lineage spike proteins……..……..…….....38
Figure 3.8: Comparison of Area Under the Curve (AUC) between SARS-CoV-2 wild type and sub-lineage spike proteins……..……..39
Figure 3.9: Neutralization plot dose-response curves for SARS-CoV-2 wil type and sub-lineage pseudoviruses……..41
Figure 3.10: Statistically significant changes in neutralization titres of SARS-CoV-2 wild type and sub-lineage pseudoviruses……..42
Figure 3.11: The fold change in neutralization titres between SARS-CoV-2 wild type and sub-lineage pseudoviruses……..43

LIST OF TABLES

Table 1.1: VOC/VOI impact on neutralization sensitivity to convalescent plasma….17
Table 1.2: World Health Organization prequalified SARS-CoV-2 vaccines and their effectiveness against SARS-CoV-2 VOCs……21

LIST OF ABBREVIATIONS

ACE2 – Angiotensin Converting Enzyme 2

AUC – Area under the curve

CHO – Chinese hamster ovary

COVID-19 – Coronavirus Disease 2019

CP – Cytoplasmic Domain DMEM – Dulbecco's Modified Eagle's Medium

DNA – Deoxyribonucleic acid

ELISA – Enzyme linked immunosorbent assay

FBS – Fetal bovine serum

FP – Fusion protein

GISAID – Global initiative on Sharing All Influenza Data

HEK – Human Kidney Embryonic

HR1 – Heptad repeat 1

HR2 – Heptad repeat 2

HIV – Human Immunodeficiency Virus

kDa – Kilo Dalton

mAb – Monoclonal antibody

NTD – N-terminal domain

Opti-MEM – Optimal minimal essential media

PCR – Polymerase chain reaction

PDB – Protein Databank

PSO – Post symptom onset

PEI-MAX – Polyethylenimine hydrochloride max

RBD – Receptor binding domain

RBM – receptor binding motif

RCF – Relative centrifugal force

RLU – Relative light unit

RPM – revolutions per minute

SARS-CoV-2 – Severe Acute Respiratory Syndrome Coronavirus 2

SDS-PAGE – Sodium dodecyl sulphate polyacrylamide gel electrophoresis

SEC – Size exclusion chromatography

SNPs – Single nucleotide polymorphisms

TM – Transmembrane domain

TMB – 3,3'5,5'-Tetramethylbenzidine

WT – Wild type

CHAPTER ONE: LITERATURE REVIEW

1.1 The SARS-CoV-2 Pandemic

Severe Acute Respiratory Syndrome Coronavirus 2 (SARS-CoV-2) that causes Coronavirus Disease 2019 (COVID-19) was first detected in Wuhan, China in December 2019 and has since led to a global public health crisis (1,2). As of 21st January 2022, over 340 million SARS-CoV-2 cases and 5.5 million deaths from COVID-19 have been reported globally with Africa accounting for over 7.9 million cases (3).

South Africa has experienced four SARS-CoV-2 epidemiological waves **(Figure 1.1)** with 3.5 million confirmed cases and over 93 000 deaths as of 21st January 2022 (3).

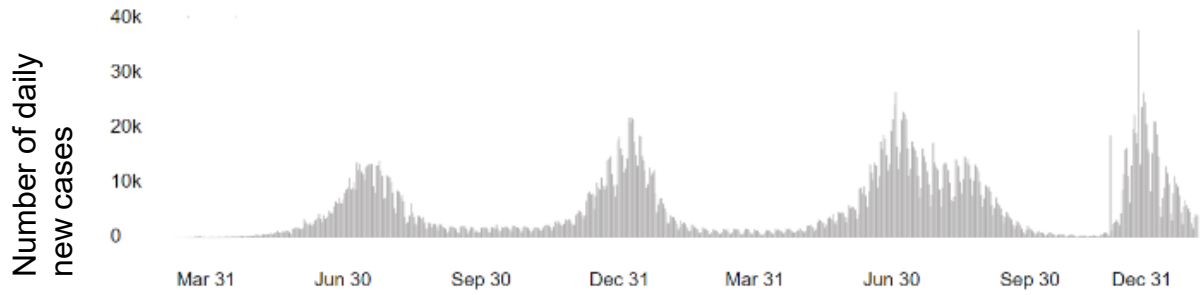

Figure 1.1:Epidemiological Waves of SARS-CoV-2 in South Africa. The graph shows the number of new cases per day in South Africa from the 5th of March 2020 to the 23rd of January 2022 (3).

The mortality and morbidity caused by this virus highlights the urgent need for research towards the implementation of SARS-CoV-2 vaccines that use a range of technologies (4) as well as therapeutic interventions such as monoclonal antibody (mAb), convalescent plasma (5,6) and drug therapies (7,8). The pandemic has been further complicated by the emergence of variants of concern (VOCs) that may reduce vaccine effectiveness, increase virulence and transmissibility (9). VOCs emerge as a result of viral evolution. Therefore, understanding the effects of vaccination and prior infection on viral evolution is essential in navigating the pandemic as they significantly shape the immune environment at the individual and population level.

1.2 SARS-CoV-2 genome and spike glycoprotein structure

SARS-CoV-2 is a positive sense single stranded RNA virus that belongs to the genera of *Betacoronaviruses*. The genome size is approximately 30 kilobase pairs in size and codes for 16 non-structural proteins. It is an enveloped virus with its genome packaged within a capsid. The envelope proteins and the spike glycoproteins cover the

nucleocapsid protein and are located on the surface of the virion (10–12). Most SARS-CoV-2 vaccines are based on the spike glycoprotein as it mediates entry into host cells and therefore blocking this protein will prevent infection (13). The spike glycoprotein is encoded by the *s* gene and consists of 3 protomers (14). Each protomer contains an S1 and an S2 subunit. The N-terminal domain (NTD) and the receptor-binding domain (RBD) that engages the host cell receptor are located on the S1 subunit **(Figure 1.2)**. The fusion protein (FP), heptad repeat 1 (HR1), heptad repeat 2 (HR2), transmembrane domain (TM)and cytoplasmic domain (CP) are located on the S2 subunit. The S2 subunit is essential for fusion with the host plasma membrane following S1 and Angiotensin Converting Enzyme 2 (ACE2) receptor binding on host cells (15). Of note, SARS-CoV-2 requires cleavage at the S1/S2 of the spike glycoprotein before viral membrane fusion with the host cell preceding entry. This cleavage is mediated by furin (16).

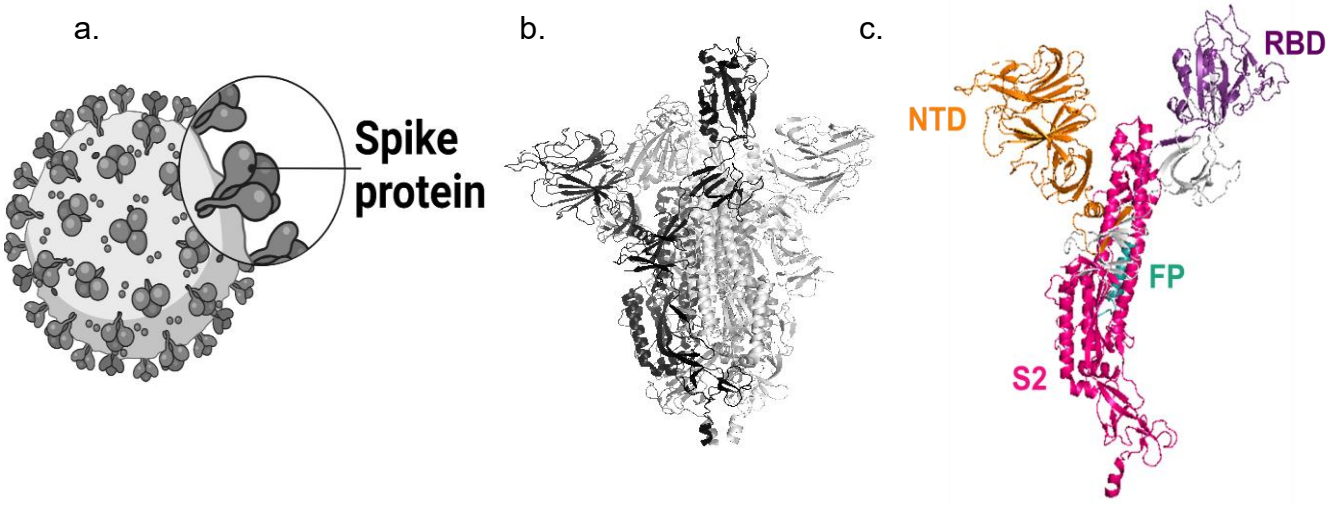

Figure 1.2: Structure of the SARS-CoV-2 spike glycoprotein (**a**) Schematic of the SARS-CoV-2 virion. Spike glycoproteins are shown protruding from the virus surface (created with BioRender.com) (**b**) The spike protein trimer is composed of three protomers (black, dark grey, and light grey). Each protomer is composed of a S1 (residues 1 - 679) and S2 subunit (residues 680 - 1273). (**c**) One protomer of the SARS-CoV-2 spike protein highlighting the location of the NTD (orange), RBD (purple), FP (teal), and S2 region (pink) (17). The SARS-CoV-2 structure was obtained from the protein databank (PDB ID:7DK3) and analysed using Pymol version 2.4.1.

1.3 Humoral immune response to SARS-CoV-2

SARS-CoV-2 S1-specific IgM and RBD IgM peak at approximately 21 days post symptom onset (PSO). RBD-specific, S1 and S2 IgG antibodies peak at approximately 28 and 33 days PSO, respectively, with asymptomatic and non-severe COVID-19 patients having significantly lower levels of anti-spike IgG response than individuals with severe illness (18). Furthermore, viral neutralization was associated with S1-specific IgA as well as RBD-specific IgA and IgG responses suggesting an important role for mucosal immunity in COVID-19 disease (18). RBD-specific IgA responses occur as early as 7 days with peak titres approximately three weeks PSO (19). RBD-specific IgA occurs earlier than RBD-IgM and wanes shortly after becoming undetectable after 1 month (18,19). Anti-spike IgG levels remained stable for at least 6 months with studies reporting that over 90% of convalescents maintain sero-positivity within a six to eight-month period post infection. Anti-SARS-CoV-2 spike IgA was shown to wane by as early as 12 weeks (20).

Humoral responses following vaccination have been characterized, One study showed that anti-SARS-CoV-2 IgG was elicited by vaccination in all vaccinees regardless of previous history of disease, However, individuals without previous history of disease had increased IgM and IgA antibody levels after primary immunization. Furthermore, after a single dose of an mRNA based vaccine, antibody levels were significantly higher in individuals who had a history of COVID19 compared to their counterparts who had no history of the disease. Notably, humoral responses were similar among both groups after administration of the second dose (21).

1.3.1 Neutralizing antibodies against the SARS-CoV-2 spike glycoprotein

Although binding antibodies may mitigate disease via Fc-effector function (22), a subset of anti-spike SARS-CoV-2 antibodies is able to prevent infection as they have neutralizing activity. These antibodies target epitopes on the S1 and S2 subunits of the spike protein and prevent infection by various mechanisms including blocking receptor binding or inhibiting membrane fusion (23). The S1 subunit elicits the majority of neutralizing antibodies with most targeting the RBD (24). Anti-RBD antibodies have been classified into four different classes **(Figure 1.3)**.

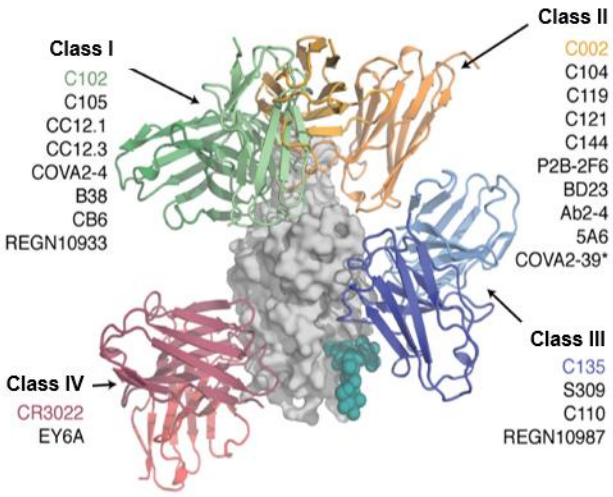

Figure 1.2: Classification of antibodies based on location of epitope on RBD of the spike glycoprotein. RBD Class I (light green) and Class II (orange) antibodies block the ACE2 binding site. RBD Class III (navy blue) and Class IV (red) antibodies bind to sites outside the ACE2 receptor binding site. Figure adapted from Barnes et. al (25).

RBD Class I antibodies block binding to the ACE2 receptor when the RBD is in the open conformation. RBD Class II antibodies neutralize SARS-CoV-2 by blocking the ACE2 binding site when the RBD is in an open or closed state. RBD Class III antibodies neutralize the virus by binding to sites outside the ACE2 receptor binding site, and are able to bind to both open and closed conformations of the RBD. RBD Class IV antibodies do not inhibit ACE2 binding and only bind when the RBD is in an open conformation (25). In convalescent plasma elicited by the original wild type strain, the dominant antibodies are Class I or Class II antibodies (26,27). Less is known about the immunodominace hierarchy in infections by other variants.

NTD-directed neutralizing antibodies recognize conformational epitopes on designated loops, particularly the N1 loop spanning residues 14 to 26, N2 loop spanning residues 67 to 79, N3 loop spanning residues 141 to 156, N4 loop spanning residues 177 to 186, and N5 loop spanning residues 246 to 260 (28). The N1, N3, and N5 loops **(Figure 1.4)** have been referred to as the NTD-supersite as most potent anti-NTD antibodies including COV2-2676, COV2-2489 (29), S2L28, S2M28, S2X333 (30), and 4A8 (28) recognize epitopes within these loops (31). This supersite is largely glycan free and positively charged while antibody paratopes are negatively charged (31). These antibodies facilitate neutralization by blocking both the fusion of the virus to the host cell membrane and the post-virus attachment step (31).

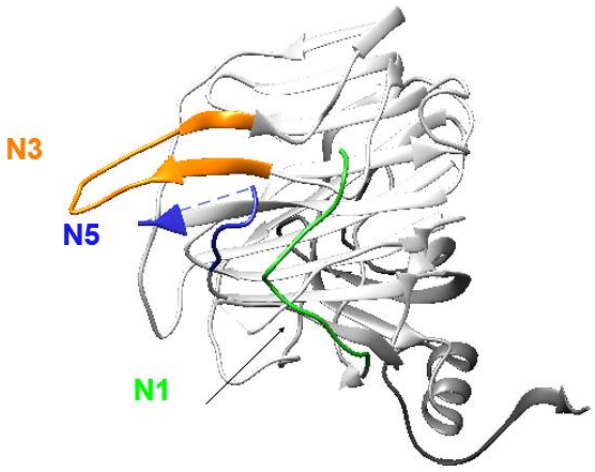

Figure 1.3: SARS-CoV-2 NTD structure. A schematic of the SARS-CoV-2 NTD region. The N1 loop is shown in green. The N3 loop is shown in orange and the N5 loop is shown in blue (26). The SARS-CoV-2 structure was obtained from the protein databank (PDB ID:7DK3) and analysed using Pymol version 2.4.1.

Furthermore, mutations to specific residues within the NTD supersite are reported to drive antibody escape. For instance mutations to spike residue positions 146, 147, and 150 (N3 loop) may disrupt salt bridges and hydrogen bonds that form during the binding of neutralizing mAb 4A8. Mutations at residue positions 246 and 248 (N5 loop) may impact spike binding to the Complementarity-determining region 1 of the 4A8 mAb (28). Although S2-specific neutralizing antibodies are rare, they have been isolated (24). Pan-coronavirus cross-reactive S2-specific antibodies have also been isolated (32) although these mAbs are limited to high binding reactivity and not neutralization (33).

1.4 SARS-CoV-2 spike evolution and the emergence of VOC/VOIs

Region-specific lineages first emerged and did not differ from the ancestral Wuhan strain by more than twelve single nucleotide polymorphisms (SNPs) (34). These lineages were replaced by the D614G lineage by March 2020. The D614G lineages conferred greater replicative fitness by increasing furin cleavage efficiency and the ratio of open to closed spike protein trimers that interact with the ACE2 receptor (34,35). In addition, individuals infected with the D614G variant had increased viral load (36). Other SNPs that emerged include the S477N and the N439K substitution that enhanced viral fitness and ACE2 binding while the latter further mediated escape from neutralizing monoclonal antibodies and convalescent plasma (37,38). In South Africa, 42 SARS-CoV-2 phylogenetic lineages were in circulation before the peak of

the 1st epidemiological wave with 16 of the lineages first being identified in South Africa (39). The three largest lineages were the C.1, B.1.1.54 and B.1.1.56 lineages that descended from a single ancestral strain and resulted in the greatest number of transmissions. All the defining non-synonymous mutations within these lineages occur outside the spike protein (39).

The SARS-CoV-2 virus is continuously evolving and has resulted in the emergence of VOCs. Similar to VOCs, variants of interest (VOIs) - SARS-CoV-2 viral genomes with distinct mutational profiles that affect transmission, diagnostic and immune profiles – have emerged but are still limited in prevalence. By late November 2021, the WHO declared five variants as VOCs (40) and other variants as variants of interest (VOI) that originated in different geographic regions across the globe (**Table 1.1**) (41). When VOCs were compared, the Alpha VOC is less associated with reduced sensitivity to neutralization by convalescent plasma when compared to the Beta/Gamma VOCs (42). However, the Delta variant showed a 4-fold reduction in neutralization sensitivity when compared to the Apha Variant (43). Sera from individuals infected with the Beta SARS-CoV-2 variant were able to neutralize the Gamma variant (44). New lineages continue to emerge, for instance, the C.1.2 (45) lineage and the Omicron variant (46) that are characterized by a combination of mutations including some that have not previously been observed. Within the viral spike protein, the C.1.2 lineage has the R190S, D215G, N484K, N501Y, H655Y and T859N substitutions and the Y144, L242-A243 deletions may be present in VOCs/VOIs. It also is defined by C136F, Y449H and N679K mutations that may improve replicative viral fitness and drive antibody escape (45). This variant has several mutations (T95I, S477N, T478K, N501Y, D614G, P681H, K417N) that are shared among VOCs/VOIs and a larger number that are unique to itself (A76V, Y145del, G339D, N440K, G446S, E484A, Q493R, G496S, Q498R, Y505H, T547K, H655Y, N679K, N764K, D796Y, N856K, Q954H, N969K, L981F). Of the 23 mutations in the spike protein (46), the Omicron variant has 15 mutations within the RBD. Of these 15 mutations, 10 mutations are located within the receptor binding motif (RBM) of the spike protein (47,48) which are the actual residues of the spike that are in contact with the ACE2 recptor during binding and entry. Some mutations within the variant have unknown individual and combined phenotypic characteristics (46). The variant largely escapes from immune responses elicited from infection and vaccination due to the increased number of mutations in the spike protein that may result in the loss of antibody binding and interaction (40).

Evolutionary changes in SARS-CoV-2 have implications for strategies such as vaccination and immunotherapies. Notably, some vaccine boosters are being adapted to accommodate mutated spike antigens (49). Despite the fact that the variant demonstrated a 22-fold reduction in neutralization by BNT162b2 vaccine elicted plasma, the vaccine was shown to retain effectiveness against the Omicron VOC (50). The evolutionary changes within the spike warrant the continuous monitoring of viral evolution and assessment of the phenotypic impacts these can have in the context of the immune responses that exist within populations. SARS-CoV-2 convalescent plasma has been used throughout the pandemic to evaluate the effectiveness of humoral responses in viral neutralization. Convalescent plasma from different variants has been used to determine cross-reactivity and changes in neutralization sensitivity between ancestral strains and emerging VOCs to evaluate the likelihood of re-infection and potential impacts on vaccine effectiveness (51–57).

Table 1.1: VOC/VOI impact on neutralization sensitivity to convalescent plasma

VOC	Lineage	Spike Mutations	(Fold change between WT and VOC)
Alpha	B.1.1.7	DEL69-70, DEL144, N501Y, A570D, D614G, P681H, T716I, S982A, D1118H (58)	2.9-fold lower▪ (51) 1.6-fold lower• (52)
Beta	B.1.351	L18F, D80A, D215G, DEL241-243, K417N, E484K, N501Y, D614G, A701V, (53)	13.3-fold lower▪ (53)
Gamma	P.1	L18F, T20N, P26S, D138Y, R190S, K417T, E484K, N501Y, D614G, H655Y, T1027I, V1176F (59)	6.7-fold lower • (52)
Delta	B.1.617.2	T19R, DEL156-157, R158G L452R, T478K, D614G, P681R, D950N (60)	3-fold lower$^{\Delta}$ (54)
Omicron	B.1.1.529	A67V, T95I, Y145D, L212I, G339D, S371L, S373P, S375F, K417N, N440K, G446S, S477N, T478K, E484A, Q493R, G496S, Q498R, N501Y, Y505H, T547K, D614G, H655Y, N679K, P681H, N764K, D796Y, N856K, Q954H, N969K, L981F, Del H69/V70, DelG142/V143/Y144, DelN211, and insertion (EPE) at position 214 (61)	4–6-fold lower $^{\Delta}$ (62)
VOI	**Lineage**	**Spike Mutations**	**(Fold change between WT and VOI)**
Eta	B.1.525	Q52R, A67V, DEL69-70, DEL144, E484K, D614G, Q677H, F888L (63)	
Iota	B.1.526	L5F, T95I, D253G, E484K, D614G, A701V (64)	3.8-fold lower$^{\Delta}$ (55)
Kappa	B.1.617.1	E154K, L452R, E484Q, D614G, P681R, Q1071H (65)	1.8-fold lower$^{\Delta}$ (54)
Lambda	C.37	G75V, T76I, Δ246-252, D253N, L452Q, F490S, D614G, T859N, (66)	3.3-fold lower$^{\Delta}$ (56)
Mu	21H/B.1.621	T95I, Y144S, Y145N, R346K, E484K, N501Y, D614G, P681H, D950N (67)	12.4-fold lower$^{\Delta}$ (57)

• Relative to SARS-CoV-2 lineage B.1, clade 20A.EU1
▪ Relative to SARS-CoV-2 lineage Victoria (Victoria (SARS-CoV-2/ human / AUS/ VIC01/2020)
$^{\Delta}$ Relative to D614G WT

The Alpha variant is susceptible to neutralization by D614G convalescent sera (68) and had negligible impact on vaccine efficacy (69). The Gamma variant demonstrated partial loss of neutralization against both convalescent plasma and Pfizer vaccine sera (70). Studies showed that the Beta SARS-CoV-2 variant had a 9-fold reduction in neutralization sensitivity to SARS-CoV-2 D614G convalescent plasma, while a 10-fold

reduction in neutralization was also observered when vaccine sera were assessed for neutralization sensitivity against the SARS-CoV-2 D614G lineage (71). The Delta VOC showed a 3-fold reduction to convalescent plasma (54) and a 5-fold reduction to sera from vaccine recipients (72,73).

The SARS-CoV-2 VOCs share several mutations that affect ACE2 receptor binding or antibody binding and neutralization. For instance, The N1, N3 loop and N5 loops of the NTD commonly possess antibody escape mutations (74). For example the L18F mutation located in the N1 loop is associated with escape from several NTD-directed mAbs (75). Several deletions have also been characterized, for instance, the deletion in the N3 loop at residue 144, which have been associated with antibody escape (76). In the RBD, the mutation N501Y enhances binding of the spike to the human ACE2 receptor increasing viral transmissibility (76,77). The K417N and E484K/Q mutations are associated with antibody escape (57,78). The K417N RBD mutation abolishes salt-bridge interactions between both the spike protein and the human ACE2 receptor and the spike protein and epitopes on mAbs e.g. CB6 (79). The RBD E484K mutation is associated with increased neutralization resistance by SARS-CoV-2 convalescent plasma and vaccine sera (80) as mutations result in the loss of antibody epitope recognition (27). Furthermore researchers noted that these three RBD mutations in combination have unique conformational changes that increase contact of the spike RBD with the ACE2 receptor resulting in greater binding affinity (81). The Beta variant has these mutations which lead to both immune escape and increased ACE2 binding **(Table 1.1)** (26,53). A notable mutation in VOC/VOIs is the L452R substitution present in the Delta VOC and, Kappa and Lambda VOIs. It increases infectivity by stabilizing the interaction between the viral spike protein and the human ACE2 receptor. Furthermore, antibodies show reduced binding and up to 4-fold reduction in neutralization attributable to conformational changes induced by the mutation (82). SARS-CoV-2 strains with mutations at spike residue position L452R were found to have reduced neutralization titers against SARS-CoV-2 convalescent plasma and vaccine sera (83).

Mutations may affect binding and neutralization across numerous RBD antibody classes **(Figure 1.5)** (27) and therefore antibody escape from multiple classes may result in one VOC/VOI. For instance, the Mu VOI contains mutations that are known to affect both class II (E484K) and class III (R346K) antibodies as well as mutations within the NTD supersite (Y144S, Y145N) (57).

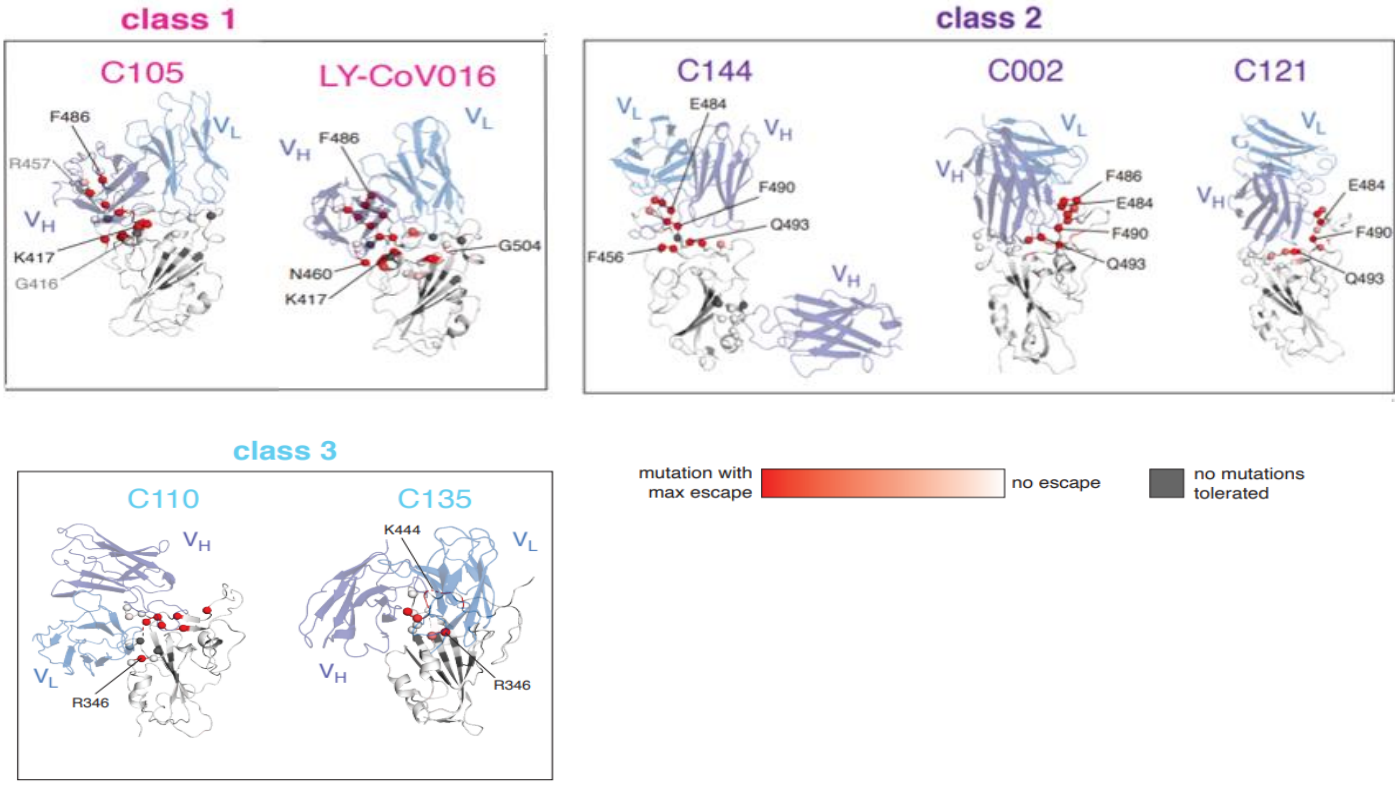

Figure 1.4: Mutations affecting antibody classes. Schematic representation of antibody classes with respective antibodies showing shared SARS-CoV-2 spike epitopes implicated in antibody escape (red) following mutation. Class I antibodies are labelled in magenta, class II antibodies are labelled in purple, and class III antibodies are labelled in light blue. Residues that do not tolerate mutations are indicated in grey. Figure taken from Greaney et. al (27).

Other notable mutations have been reported including the P681H/R (84) mutations which are associated with increased spike furin cleavage resulting in increased viral replication fitness and these mutations are found in Alpha, Delta, Kappa and Mu VOC/VOIs (84). In addition to improving cell mediated entry by improved spike cleavage, these mutations are reported to increase spike-mediated cell fusion facilitating infection of cells even in the presence of neutralizing antibodies (85). This may provide insight into the continued spread of the Delta variant despite the ongoing immunization efforts.

1.5 SARS-CoV-2 vaccine efficacy against VOCs/VOIs

Since the rapid development of SARS-CoV-2 vaccines begun in 2020, several vaccines have been licensed for use and are in use in vaccination programs (86,87). The impact of combined mutations within VOCs may be assessed by determining whether there are changes in vaccine effectiveness before and after the emergence of

VOCs **(Table 1.2)**. For instance, researchers noted that the overall vaccine effectiveness of the COVID-19 vaccines against infection was 91%, however after the emergence and widespread of the SARS-CoV-2 Delta variant the vaccine effectiveness declined to 66% (88). One study estimated the vaccine effectiveness of the BNT162b2 vaccine against infection to be 88% before the emergence of VOCs (89). Other studies showed that the BNT162b2 vaccine effectiveness against infection with the Beta variant was 75% (90) and even lower (53%) for the Delta variant (91). Studies have shown the decline in vaccine effectiveness due to circulating SARS-CoV-2 variants that are resistant to immune responses elicited by infection or vaccination (76).

Table 1.2: World Health Organization prequalified SARS-CoV-2 vaccines and their effectiveness against SARS-CoV-2 VOCs

Vaccine code name	Manufacturer	Vaccine Efficacy against WT	Vaccine effectiveness against ancestral strains	Vaccine Effectiveness against VOC	
BNT162b2	Pfizer/BioNTech	95%^(92,93)	72%+$^{\Delta}$ United Kingdom (94)	Alpha	89%^˚ (95)
			60% +$^{\Delta}$ Israel (94)	Beta	75.0%$^{+}$˚(90)
			77.6%+$^{\Delta}$ United States (89)	Beta/ Gamma	84%^˚(95)
			88.8%+˚ United States(89)	Delta	53.5%$^{+}$˚(91) 89.7%˚∞ (91)
AZD1222	Astrazeneca	62.6%^ (92)		Alpha	37%$^{\Delta}$ (96)
				Delta	81·5˚∞ (97) 79·2 $^{\Delta}$∞ (97)
Ad26.COV2.S	Johnson & Johnson	66.%+(92,98)		Delta	51%$^{+}$˚(98)
mRNA-1273	Moderna	94.% (93) 95%^(92)	88.9% United States(89)	Alpha	92%^˚ (95)
			96.3%+˚ United States(89)	Beta	96% ˚$^{+}$ (99)
				Delta	84.8%$^{+}$˚ (66) 100.0% ˚∞ (66)
BBIBP-CorV	Sinopharm			Delta	59.0%˚$^{+}$ (100) 70.2%)^˚(100)

˚ fully vaccinated
$^{\Delta}$ partial vaccination
$^{+}$ Vaccine efficacy against infection
∞ Vaccine effectiveness against severe disease
^ Vaccine effectiveness against symptomatic infection

1.6 Study Aims and Objectives

SARS-CoV-2 is continually evolving and immune responses elicited by vaccination and infection may be less effective in providing protection from infection with future VOC/VOIs. Public health measures such as vaccination and monoclonal antibody treatments rely heavily on what is known about the viral sensitivity to immune responses. Therefore, paired genomic surveillance and testing sensitivity to immune responses elicited by vaccination or infection are crucial. This study was undertaken to identify and probe the effect of spike mutations detected in South Africa on neutralization by SARS-CoV-2 directed antibodies in convalescent plasma.

The specific objectives of this study were to:

1. To identify locally relevant mutations within SARS-CoV-2 spike gene sequences and utilize site-directed mutagenesis to introduce these mutations into recombinant spike protein and pseudovirus constructs.
2. To generate and characterize soluble wild type and mutated SARS-CoV-2 spike trimer proteins by mammalian cell expression, chromatography-based protein purification and sodium dodecyl-sulfate polyacrylamide gel electrophoresis .
3. To assess the effect of mutations on binding and neutralization of SARS-CoV-2 directed antibodies in convalescent plasma by enzyme-linked immunoassay and pseudovirus neutralization assays.

CHAPTER TWO: METHODS

2.1 Cohort description

Plasma samples used in this study were obtained from an observational cohort study that evaluated COVID-19 outcomes in both HIV-seropositive and HIV-seronegative individuals at the Steve Biko Hospital in Johannesburg. Of the samples obtained for use in the parental study, forty-two samples were collected prior to the 15th of September, 2020. This subset of samples was included in this study to ensure that the convalescent plasma obtained was from individuals that were infected with strains – likely ancestral D614G strains – that circulated prior to the emergence of the Beta VOC. An ongoing SARS-CoV-2 household transmission study (HTS) in Soweto, Gauteng and Jouberton, Mpumalanga enrolled SARS-CoV-2 positive participants who presented at healthcare centres with mild or asymptomatic disease that did not require hospitalization. Each participant's household was subsequently enrolled in the study and followed for a period of six to eight weeks. Three nasopharyngeal swabs were collected at two-week intervals by researcher collaborators from the National Institute for Communicable Diseases (NICD) of the National Health Laboratory Services (NHLS) in the aforementioned study. Samples from SARS-CoV-2 positive participants were collected during December 2020 and were sequenced by the same researchers.

2.2 Ethical Approval

The principal investigator of the parent study (entitled "Observational cohort study of the natural progression of COVID-19 in a high HIV prevalence area") obtained ethical approval from the Faculty of Health Sciences, University of Pretoria, Research Ethics Committee for the collection of participant data, samples, and for these research studies (Ethics reference number: 247/2020).

Sequences for the identification of SARS-CoV-2 lineages were obtained from the SARS-CoV-2 household transmission study (HTS) in Soweto, Gauteng and Jouberton, Mpumalanga. Ethical clearance for the study was obtained from the University of the Witwatersrand, Human Research Ethics Committee, (Ethics clearance certificate number: M2008114).

Ethics clearance for this sub-study was obtained from the Faculty of Health Sciences, Human Research Ethics Committee, University of the Witwatersrand (Ethics clearance certificate number: M2011190).

2.3 Identification of sub-lineages

SARS-CoV-2 sub-lineages were identified from positive samples in the HTS study that was wholly conducted by our collaborators at the NICD. Ninety-five sequences were obtained and analysed in this study. The lineage that each sequence belonged to was determined using the Pangolin COVID-19 Lineage Assigner (https://pangolin.cog-uk.io/) and Nextclade version 1.1.0 (https://clades.nextstrain.org/) tools. The local and global frequency of mutations in each sub-lineage was determined by assessing sequences from the GISAID database (https://www.gisaid.org/).

2.3 Protein Structural Analysis

UCSF Chimera version 1.15 and ICM Browser version 3.9 were used to visualise cryo-electron microscopic structures of SARS-CoV-2 in complex with the ACE2 receptor protein or relevant monoclonal antibodies. Interactions between proteins were observed and changes in structural interactions were observed after mutating relevant residues in the protein structure *in silico*.

2.4 Site Directed Mutagenesis

The Quick Change Lightning Site-Directed Mutagenesis Kit was used to introduce mutations into a plasmid encoding a SARS-CoV-2 soluble spike, that contains six proline substitutions that stabilize the protein in a prefusion state. This enables high expression as well as stability during storage, freeze-thaw cycles and heating (101). The Hexapro spike plasmid, which contains a Kanamycin antibiotic resistance gene and a his-tag was obtained from Jason McLellan (University of Texas). Mutagenesis was also used to introduce mutations into SARS-CoV-2 spike plasmids that have been codon optimized for expression in Chinese hamster ovary (CHO) cells (26) and used to generate pseudoviruses.

Synthetic oligonucleotide primers were designed using the Agilent QuikChange Primer Design tool (www.agilent.com/store/primerDesignProgram.jsp). The double-stranded-DNA template, mutagenic primers, dNTPs, QuikChange Lightning buffer, QuikChange Lightning enzyme, QuikSolution Enzyme, double distilled H_2O and mutagenic primers were added according to protocol. Mutagenic primers were used to introduce single-point mutations into the wild type plasmids. The PCR of 1 cycle of 95˚C for 2 minutes, 30 cycles of 95˚C for 20 seconds, 55˚C for 30 seconds, 65˚C for 4 minutes 30 seconds, and 1 cycle of 65˚C for 5 minutes was used to denature templates, and subsequently anneal and extend the mutagenic primers resulting in the amplification of the

recombinant protein-coding sequences and pseudovirus plasmids with desired single point mutations. *DpnI* enzyme was used to digest the parental methylated DNA leaving only synthesized mutant plasmids with staggered nicks that were subsequently used to transform XL-10 Ultracompetent *E*. coli cells.

2.5 XL-10 Gold Ultracompetent *E. Coli* Cell Transformation

According to the manufacterer's protocol, two microliters (ul) 2-Beta-mercaptoethanol was added to a 45 µl aliquot of XL-10 Gold Ultracompetent *E. Coli* cells to inactivate surface nucleases. *DpnI* enzyme treated DNA (2µl) was added and incubated for 30 minutes before heat shocking the cells at 42˚C to ensure migration of plasmid DNA into the cells through pores. A 500 µl volume of Super Optimal Broth was added and cells were incubated for 1 hour with shaking at 200 – 250 revolutions per minute (rpm) to allow for the recovery and stabilization of cells. Cells transformed by soluble spike protein-coding plasmids and pseudovirus spike-coding plasmids were cultured on LB agar plates containing Kanamycin and Carbenicillin antibiotic, respectively. After 16-24 hours a colony was inoculated into 15ml LB broth and further incubated at 37˚C with shaking (200 – 250 rpm).

2.6 DNA Extraction

Mutated DNA was extracted from *E. coli* cells using QIAGEN® Plasmid Plus Maxi Kit and the ZymoPURE™ II Plasmid Maxiprep Kit as per manufacturer instructions. Cells were harvested from bacterial cultures that were grown in 15 ml of LB broth at 37˚C with shaking for 16-24 hours after transformation by mutated plasmids. After centrifugation at 2504 relative centrifugal force (rcf) or g force for 5 minutes at 15 - 25˚C, bacterial pellets were resuspended into the lysate buffer solution that releases nucleic acid from the bacterial cells. A binding buffer was used to optimize the binding of nucleic acids to the column. Subsequently, washing buffers were used to remove contaminants without interfering with the bound plasmid DNA. High quality plasmid DNA was eluted using 10 mM TrisCl (pH 8.5), or 0.1 mM EDTA (pH 8.5) and the concentration of DNA was determined using the Nanodrop-1000 using spectrophotometry to quantify nucleic acids by determining the amount and pattern of ultraviolet light absorbed at a wavelength of 260 nm.

2.7 DNA Sequencing

Extracted DNA was evaluated for successful mutagenesis by Sanger sequencing. The ABI PRISM BigDye Terminator Cycle Sequencing Ready Reaction kit and forward and reverse sequencing primers that targeted the nucleotide region with the mutation were used to sequence the plasmid insert. The polymerase chain reaction (PCR) was performed at 25 cycles of 96˚C for 10 seconds, 50˚C for 05 seconds, 60˚C for 4 minutes. The sequencing reaction was purified using a freshly prepared mixture of sodium acetate prepared by combining 8 ml of 100% ethanol and 320 µl of 3M sodium acetate. This mixture causes the precipitation of nucleic acids in the sequencing reaction solution which can further be separated by centrifugation. A 50 µl volume of the ethanol sodium acetate mix was added to each well and centrifuged for 30 minutes at 2000 rcf after mixing. Subsequently, supernatant was discarded and 100 µl of cold 70% ethanol was added to the pellet before further centrifuging for 5 minutes at the same speed. The supernatant was discarded and the pellet was dried at 65˚C for 3 minutes. Sequences were resolved on an automated genetic analyser and the chromatograms were viewed on Sequencher® (Gene Codes, version 5.4.6) to determine whether the desired mutations were obtained.

2.8 Maintenance of 293F, 293T, 293T/ACE2 cell lines

Human Embryonic Kidney (HEK) 293F, 293T, and 293T/ACE2 cells were used for the expression of soluble SARS-CoV-2 spike trimer, the production of SARS-CoV-2 spike pseudovirus, and the assessment of viral infectivity by neutralization assays, respectively.

HEK 293F suspension cells efficient for the growth of recombinant protein were maintained in Freestyle media and incubated at 5% CO2, and 37˚C with shaking (200 – 250 rpm). HEK 293T adherent cells have a SV40 origin of replication and are efficient for producing large amounts of viral particles. These cells were maintained in Dulbecco's Modified Eagle's Medium (DMEM) enriched with 10% FBS, 3% HEPES buffer and 0.5% Gentamycin and incubated at 37˚C. HEK 293T/ACE2 cells were maintained in DMEM media enriched with 10% FBS, 3% HEPES buffer, 0.5% Gentamycin and 0.03% Puromycin (3 µg/ml) and incubated at 37˚C.

2.9 SARS-CoV-2 trimer expression, purification and size exclusion chromatography (SEC)

Expression of SARS-CoV-2 trimer was carried out in HEK 293F suspension cells. SARS-CoV-2 plasmid DNA was mixed with freshly prepared 1 mg/ml Polyethylenimine hydrochloride (PEI-MAX) transfection reagent at a ratio of 1:3, in serum free culture medium, Opti-Pro. PEI-MAX forms positively charged particles with the DNA. Transportation into the cell occurs via endocytosis once positively charged complexes have been bound to negatively charged surfaces of cells (102). The transfection mix was filter sterilized using a 0.22 micron filter and added to HEK 293F seeded cells at 1 x 10^6 cells/ml in a volume of 1 litre in erlenmeyer flask the previous day. The cell culture was incubated at 37˚C, 70% humidity, 8-10% CO2 in a shaking incubator (200 – 250 rpm).

After six days, the supernatant containing the histidine-tagged SARS-CoV-2 trimers was filtered using a 0.22 micron filter to remove cells and was loaded onto a nickel sepharose column for immobilized metal affinity chromatography. The column was washed using wash buffer with a 20 mM concentration of imidazole to remove unbound proteins. Subsequently, a high imidazole containing buffer was used to elute the protein as the higher concentration of imidazole (235 mM) in the elution buffer competes with the his-tag on the protein for binding to the metal-charged resin. The protein was then concentrated in a centrifugal concentrator with a 50 000 dalton molecular weight cut-off membrane by centrifugation at 3399 rcf for approximately 30 minutes in preparation for size-exclusion chromatography (SEC).

SEC was used to separate the eluted protein by size and molecular weight. Concentrated protein was loaded onto a Hiload™ 16/60 Superdex™ 200 prep grade column equilibrated in 3mM HEPES, 150mM sodium chloride and 0.02% sodium azide buffer. SEC separates molecules based on their molecular size by filtration through a gel composed of spherical beads with pores of different sizes. Molecules of various sizes are included or excluded from the pores in the matrix allowing for separation. Molecules are eluted in decreasing order of molecular size by time as smaller molecules are obstructed by the pores of the gel matrix and take a longer time to be eluted. The fractions eluted at 42 – 55 minutes were collected and concentrated as the SARS-CoV-2 spike trimer (180 kDa) falls within the fractionation range. Aliquots were stored at - 80˚C until use.

2.11 Sodium dodecyl sulphate–polyacrylamide gel electrophoresis

Reducing and non-reducing sodium dodecyl sulphate–polyacrylamide gel electrophoresis (SDS-PAGE) were used to confirm protein size. For non-reducing and reducing SDS-PAGE, LDS sample buffer was added to protein and heated at 100˚C to allow for denaturation. 15% Beta-mercaptoethanol was used as the reducing agent. Subsequently, protein was loaded onto a Novex™ Invitrogen™ Thermo Fisher Scientific, precast polyacrylamide gel (polyacrylamide percentage: 4-12%). Novoxex Pre-Stain Sharp Molecular Marker was used to determine the molecular weight. NuPAGE MOPS SDS running buffer was used to run the gel at charge of 200 volts. PageBlue™ Protein Staining Solution was used for staining the gel which was subsequently visualized on a GelDoc reader.

2.12 Enzyme Linked Immunosorbent Assay (ELISA)

An established, in-house SARS-CoV-2 indirect ELISA assay was used to determine the presence of antibodies in convalescent plasma directed against the wild type (WT) and mutant spike proteins (103). WT and mutant SARS-CoV-2 spike protein (2 μg/ml) were used to coat a 96-well high-binding plate. After washing the plates three times in the wash buffer (1x PBS, 0.05% Tween 20) and blocking the plates with 5% skimmed milk the plasma samples (diluted to 1:100 in blocking buffer) were added to the plates. Monoclonal antibodies, diluted to a concentration of 5 μg/ml were used as positive controls (CR3022, 4A8, P2B-2F6 and CC12.23) and negative controls (Palivizumab). Samples were run in duplicate at 3-fold serial dilutions. The secondary antibody (anti-human horse radish peroxidase-conjugated antibody) was diluted to 1:3,000 in blocking buffer and added to the plates. A 1-step 3,3'5,5'-Tetramethylbenzidine (TMB) substrate was added to wells according to protocol to detect any bound antibody. The reaction was stopped using 1M H_2SO_4. The SpectraMax® ABS Plus Microplate Reader was used to measure optical density at 450nm wavelength and therefore detect binding. The area under the curve (AUC) was determined for each sample. The Friedman's test with Dunn's correction was used to compare data from each sub-lineage.

2.13 Pseudovirus production

SARS-CoV-2 pseudoviruses were prepared according to an established in-house protocol using HEK 293T cells. Filter sterilized PEI-Max at a concentration of 1 mg/ml was added to 479.0 μl of Opti-Pro media and incubated for 5 minutes according to protocol. The modified HIV proviral molecular clone pNL4 backbone with the *nef*

reading frame substituted with firefly luciferase gene was used as it lacks a functional HIV *env* allowing for the expression of SARS-CoV-2 spike proteins. The pNL4 backbone with luciferase gene (6 μg) and WT or mutant spike vector (6 μg) were added to Opti-Pro (479 μl) media according to procedure. DNA/Media mixture was transferred to the PEI/Media and the transfection reagent-DNA complex were added to HEK 293T cells previously seeded at $1x10^6$ cells in a T-75 flask and incubated for 72 hours. The supernatants were harvested and filtered using a 0.45-micron filter. The fetal bovine serum (FBS) concentration in the virus-containing culture medium was adjusted to 20% and aliquots of the virus were stored at –80°C in sterile cryogenic tubes. The dilution of virus required to yield 50 000 – 250000 relative light units (RLUs) in the assay was determined by $TCID_{50}$ titration of each batch of virus produced.

2.14 Neutralization assay

A pseudotype neutralization assay previously described (26) was used to determine whether SARS-CoV-2 antibodies present in convalescent plasma could neutralize the pseudotyped viruses that contain relevant mutations. Plasma samples from COVID-19 convalescent donors were heat-inactivated at 56°C degrees to inactivate complement proteins that may interfere with the assay. Samples were clarified by centrifuging at 2000 rcf for 10minutes. Growth media and convalescent plasma containing SARS-CoV-2 antibodies was added to flat-bottom 96-well plates and titrated in 5-fold serial dilutions. A volume of 50 µl of SARS-CoV-2 pseudovirus (at a concentration that achieved 25000 – 250000 RLU during TCID) was added to the plate and incubated for 45-90 minutes to allow antibodies to bind to the spike protein. To each well, 100 µl of 293T-ACE2 expressing cells at a concentration of 1×10^6 were added to the wells and further incubated at 37 °C for 72 hours. Subsequently, media was aspirated from wells and 1x Promega lysis buffer was added to lyse cells. Bright Glow Luciferase reagent was used to detect luciferase released by lysed infected cells as a measure of infectivity. After transfer to a 96-well black and white plate, light signals produced in each well were read by the Perkin Elmer XL luminometer and compared to the results of the cell control and virus control wells that were prepared in the same manner. Neutralization assays were run in duplicate to determine inter-assay variation. Dose-response curves were generated using GraphPad Prism (version 8.0.1). The ID_{50} which is the serum dilution that inhibits 50% of the infectivity was also determined. The Friedman's test with Dunn's correction was used to compare data between the four sub-lineages.

CHAPTER THREE: RESULTS

3.1 Sub-lineage mutations identified from SARS-CoV-2 infected individuals

Researchers in the HTS study obtained nasopharyngeal swabs from SARS-CoV-2 positive individuals participants in Soweto, Gauteng and Jouberton, Mpumalanga. Samples from SARS-CoV-2 positive participants were sequenced. The HTS study sequenced samples and grouped sequences into sub-lineages that have not previously been defined in other studies. In this study sub-lineage 1 is defined by the D215G, deletion 241-243, L452R, Y508H and D614G mutations in the spike protein. Sub-lineage 2 is defined by D80A, D215G, deletion 241-243, L452R, E484K, D614G and A701V mutations in the spike protein. Sub-lineage 3 is defined by D80A, L452R, Y508H, D614G and A701V spike protein while sub-lineage 4 is defined by D215G, L452R, Y508H, D614G and A924T mutations in the spike protein (**Figure 3.1a - d)**. Of the 95 sequences obtained by the HTS study in December 2020, five sequences (0.05%) were classified under Sub-lineage 1, one sequence (0.01%) belonged to Sub-lineage 3, and one sequence (0.01%) was identified as belonging to sub-lineage 4. No viruses belonging to Sub-lineage 2 were identified. Fifteen sequences had D80A, D215G, Del241-243, E484K, D614G, A701V mutations, however, they could not be classified as Sub-lineage 2 sequences as they did not have the L452R mutation. Sequences from sub-lineages were analysed using Nextclade clades.nextstrain.org (version 1.7.1). Sub-lineage 3 was classified under clade 19B lineage and Sub-lineage 4 was categorized as part of clade 20B. Both clade 19B and 20B have less than 10 mutations in their genome compared to the VOC/VOIs which belong to other clades that have greater than 10 mutations in their genomes **(Figure 3.1e)**. The Pangolin COVID-19 Lineage Assigner was unable to determine the pangolin lineage of all sequences in the four sub-lineages.

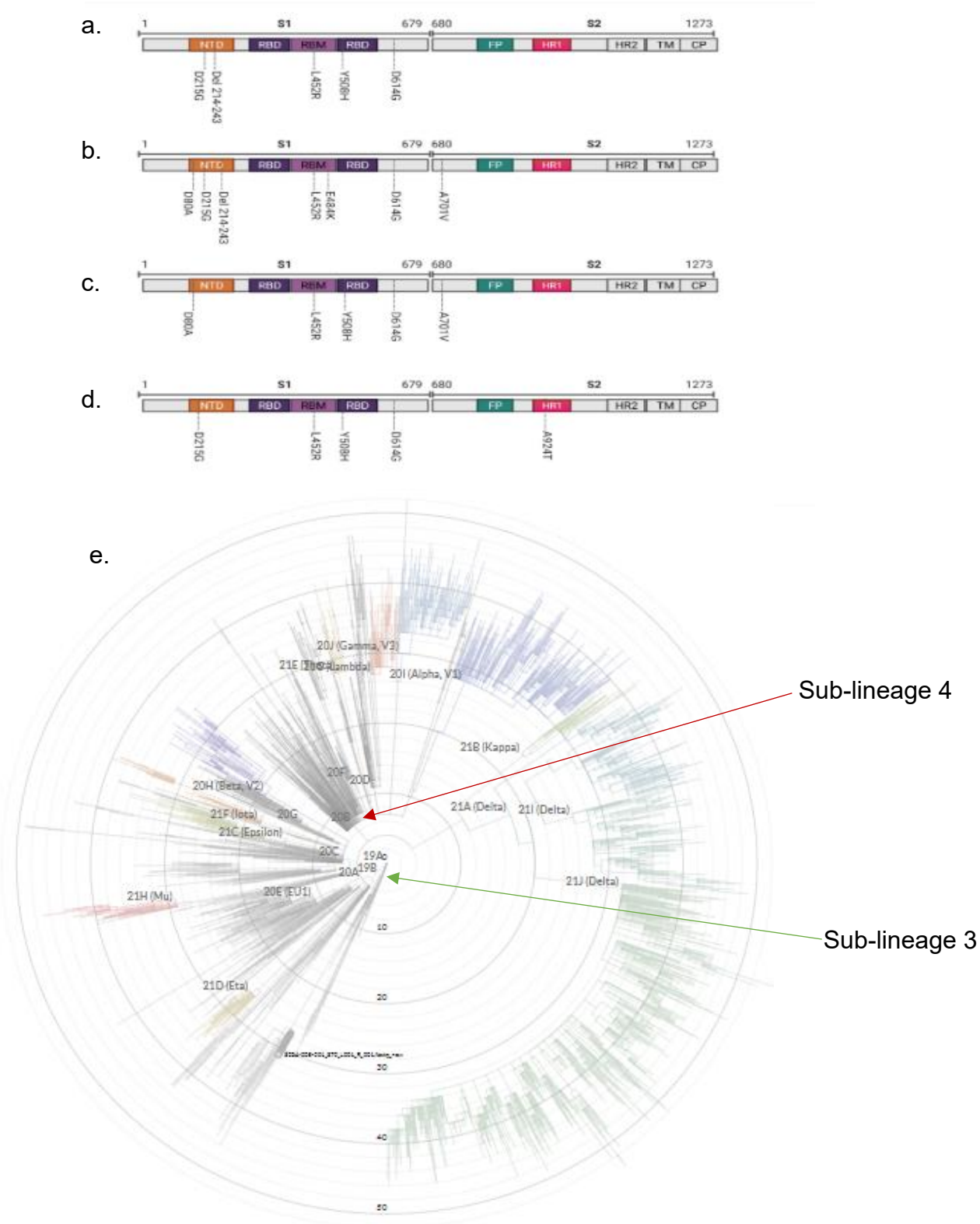

Figure 3.1: Schematic representation of the mutations in each sub-lineage and Nextclade sequence lineage assignment. The S1 and S2 demarcations are indicated. The NTD is shown in orange, the RBD is shown in purple, RBM is are shown in light purple, the FP is shown in teal, and the HR1 is shown pink. HR2, TM and CP are also shown**(a)** Mutations present in (**a**) sub-lineage 1, (**b**) sub-lineage 2, (**c**) sub-lineage 3 (**d**) sub-lineage 4. (**e**) SARS-CoV-2 global clades as shown in the radial phylogenetic tree. The number of mutations in each clade (range 0 – 50) is indicated. Distance from the reference strain represents genetic variability. Sub-lineage 3 (green) sequence belongs to the clade 19B. Sub-lineage 4 (maroon) sequence belongs to the clade 20B.

After sub-lineages were defined from the HTS study, this study utilized the GISAID database to determine the frequency of individual mutations that define the four sub-lineage of mutations evaluated in this study. The D614G mutation was found in over 98% of sequences that were deposited onto the database from across the globe. In South Africa, the D614G mutation was present in 97% of the reported sequences (**Figure 3.2**) as of 6th December, 2020. The L452R mutation was observed in approximately a third of all reported sequences both globally and locally. The A701V and E484K substitutions were also observed in a third of locally reported sequences. In addition, the D80A and D215G substitutions were observed in a quarter of locally reported sequences. All other mutations were represented in less than 25% of the reported sequences (**Figure 3.2**).

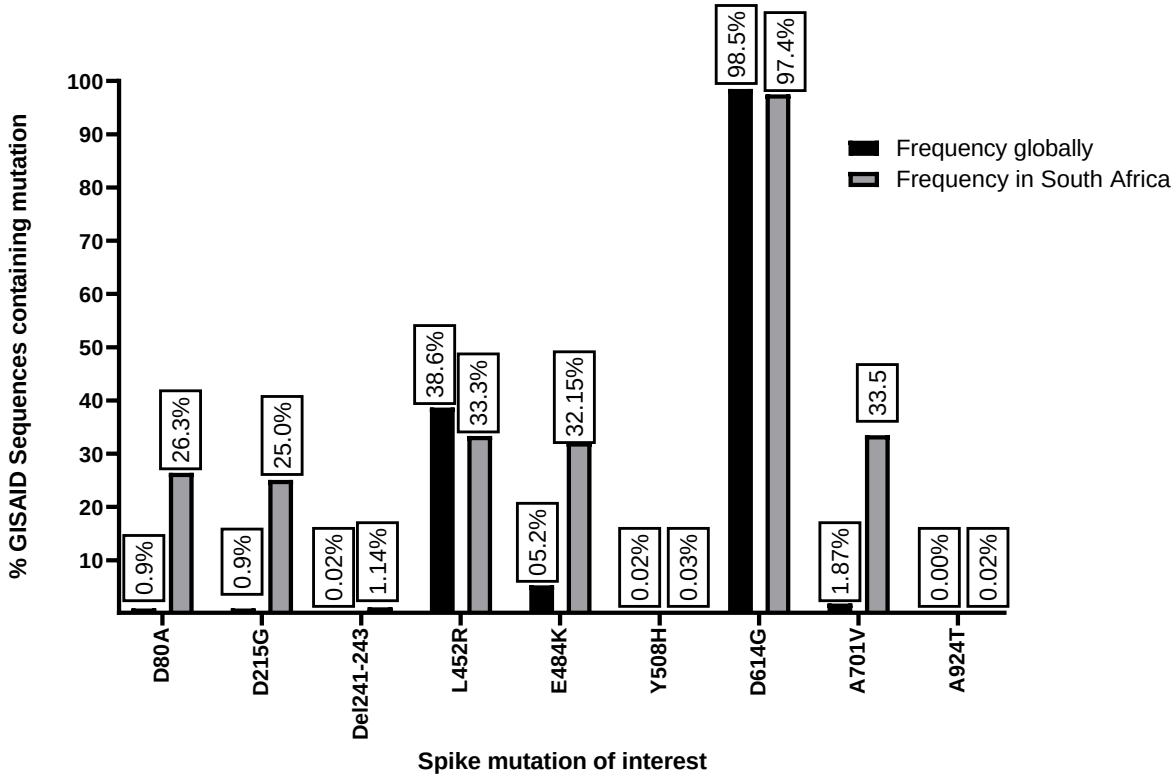

Figure 3.2: Percentage of GISAID sequences with mutations of interest. The percentage of global and local (South Africa) GISAID sequences that contain mutations of interest that define the four sub-lineages evaluated in this study is displayed. The y-axis shows the percentage and the x-axis shows the mutation of interest. Black and grey columns represent percentage of sequences globally and in South Africa, respectively.

3.2 Protein Structural Analysis

Protein modelling was used to observe the structural interactions between the SARS-CoV-2 spike protein and ACE2 receptor or monoclonal antibodies in order to determine

structural changes that result from point mutations that may have an impact on binding affinity and consequently viral infectivity and immune evasion. Cryo-EM structures of SARS-CoV-2 in complex with the ACE2 receptor protein or relevant monoclonal antibodies were obtained from the Protein Data Bank (PDB) and were visualized using UCSF Chimera version 1.15. Changes to interactions between amino acids were determined after mutating relevant residues in the protein structure *in silico*.

The L452R mutation found within the Delta, Kappa, and Lambda VOCS is also present within all sub-lineages evaluated in this study. Mutation at this residue results in a change from a non-polar, aliphatic amino acid group (leucine) to a positively charged amino acid group (arginine). Located within the receptor binding motif (RBM) of the spike glycoprotein, studies have noted that the L452R mutation increases spike protein stability and results in higher binding affinity between the spike RBD and the ACE2 receptor (104). Structural analysis within this study suggested that molecular interactions were significantly altered between the spike and the AEC2 receptor as a result of this mutation **(Figure 3.3a - b)**. P2B-F26, a Class II mAb, and the mutant spike were analysed and the residues R452 of the spike and V105 of heavy chain showed a steric clash (0.7 **Å**) **(Figure 3.3a - b)** which suggest that the binding previously seen between the two residues was abolished. The E484 residue which is located within the RBM can contact the ACE2 receptor. The substitution of a lysine changes the amino acid at that position from being negatively charged to having a positive charge. Sub-lineage 2 strains as well as the Beta, Iota, Eta, Mu VOC/VOCs carry this substitution in the spike glycoprotein. Several studies have noted that E484 spike mutations significantly affect the binding of Class II monoclonal antibodies (27). In congruence with these findings, CB6, a Class I mAb, did not show any significant change in interaction when the mutation was introduced, however, P2B-F26 showed a significant change with the loss of a hydrogen bond (2.4 **Å**) between the 484 residue of the spike and the Y34 residue of the monoclonal antibody light chain **(Figure 3.3c – d)**.

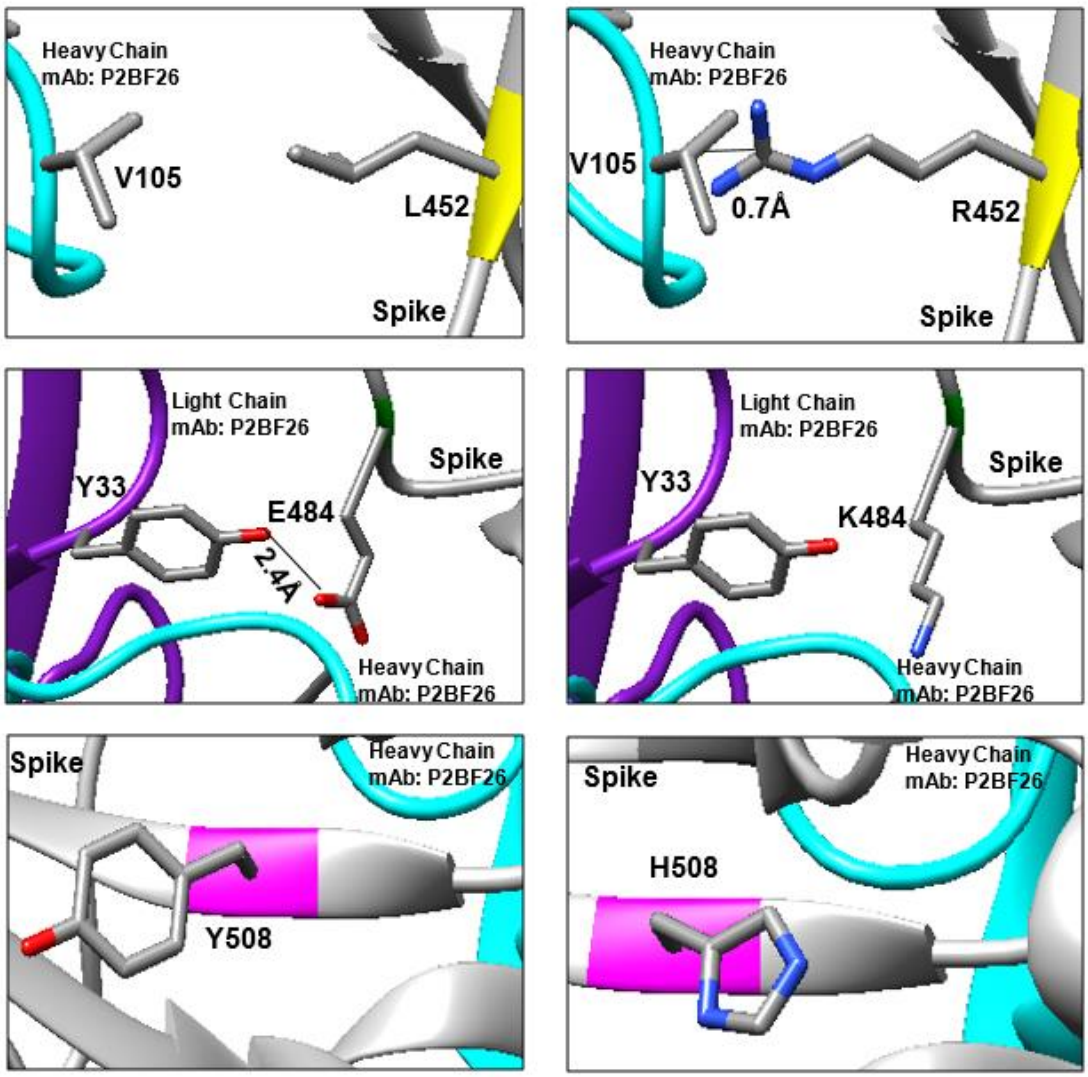

Figure 3.3: Change in protein interactions due to mutations in the spike glycoprotein (a) L452 WT and P2BF26. **(b)** R452 Mutant and P2BF26. **(c)** E484 WT and P2BF26. **(d)** K484 Mutant and P2BF26 **(e)** Y508 WT and P2BF26 **(f)** H508 Mutant and P2BF26**.** The mAb heavy chain is shown in cyan and the mAb light chain purple. The red and blue on the amino acid structures represent oxygen molecules and nitrogen molecules, respectively. Binding between residues is indicated by the black line between relevant amino acid residues.

The Y508 mutation found in Sub-lineage 1, Sub-lineage 3 and Sub-lineage 4 is located in the RBD of the spike. The substitution of the tyrosine by a histidine changes the non-polar aromatic amino acid at that position to a positively charged amino acid. This mutation has not occurred in previously described VOCs. In this study, the mutation did not show significant changes to interactions between the spike protein RBD and the ACE2 receptor, CB6, or P2B-F26 mAbs **(Figure 3.3e - f)**.

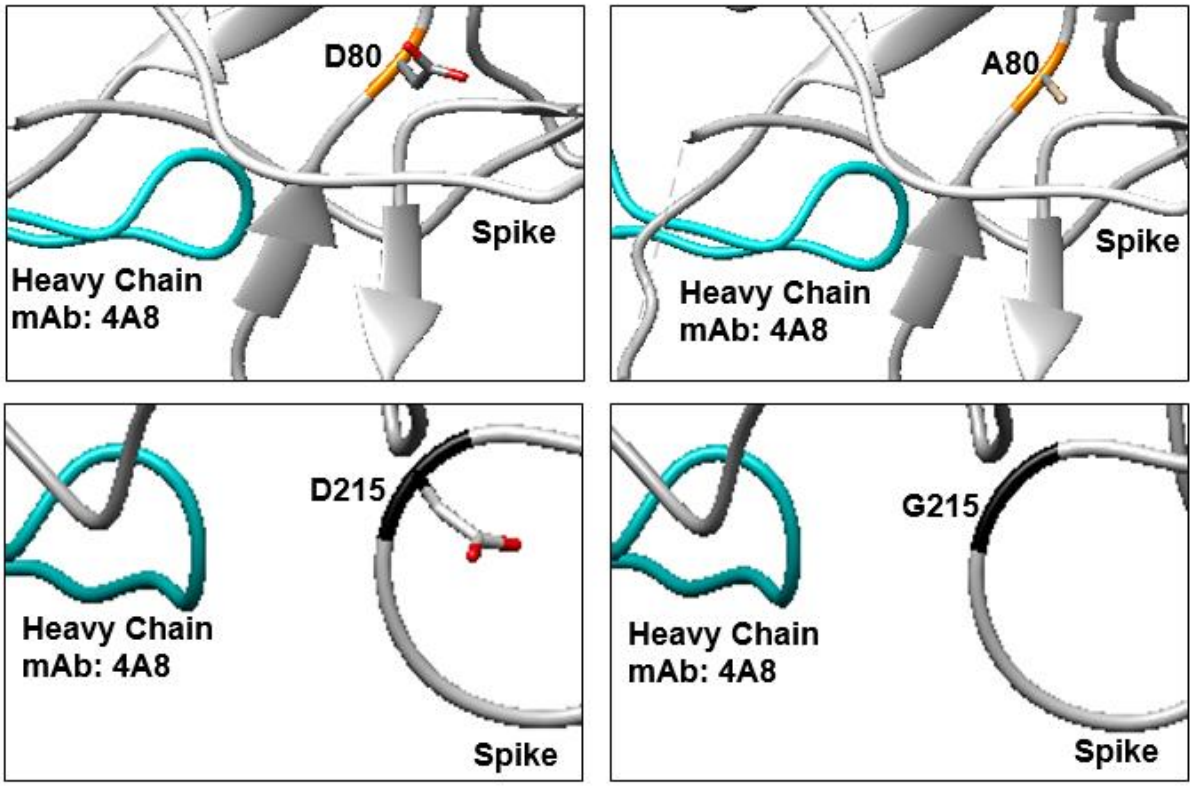

Figure 3.4: Change in protein interactions due to mutations in the spike glycoprotein (a) D80 WT and 4A8. **(b)** A80 mutant and 4A8. **(c)** D215 WT and 4A8. **(d)** G215 mutant and 4A8. The spike glycoprotein is shown in grey and the the mAb heavy chain is shown in cyan. The red on the amino acid structures represents oxygen molecules.

The D80, D215 and D241- 243 residues are located within the NTD of the spike protein. The substitution of aspartic acid by arginine at residue position 80 changes the amino acid at that position from polar a uncharged amino acid to a positively charged amino acid. Sub-lineage 2 and Sub-lineage 3 strains as well as the Beta VOCs carry this substitution in the spike glycoprotein. Studies have shown that this mutation decreases neutralization sensitivity to some NTD-directed mAbs (71). This study did not identify any significant alterations to interactions between the spike and the 4A8 mAbs **(Figure 3.4a - b)**.

The aspartic acid to glycine mutation at position 215 changes the amino acid from a negatively charged amino acid to a non-polar aliphatic amino acid. Sub-lineage 2 and Sub-lineage 4 strains as well as the Beta VOC carry this mutation. Other studies have shown that this mutation decreases neutralization sensitivity to some NTD-directed mAbs (71). The structural analysis of mAb 4A8 in complex with mutant spike did not show any significant changes in interactions (3 Å or less) were observed between the spike protein and the mAbs **(Figure 3.4c - d)**.

3.3 Sanger Sequencing

For each of the four spikes representing each of the sub-lineages, mutations were introduced into SARS-CoV-2 spike plasmids and confirmed by Sanger sequencing. The mutated spikes were compared to reference sequences to confirm the substitution of the residues and high plasmid yields were further obtained by maxiprep.

3.4 SARS-CoV-2 spike protein expression and purification

SARS-CoV-2 spike trimers with relevant mutations for each of the four sub-lineages were expressed in HEK 293F cells. Six days post-transfection, protein was harvested from the supernatant and a nickel resin column was used to purify protein trimers. Size exclusion chromatography was used to separate protein by molecular size. Proteins eluted between 44 – 54 minutes were collected **(Figure 3.5a)**.

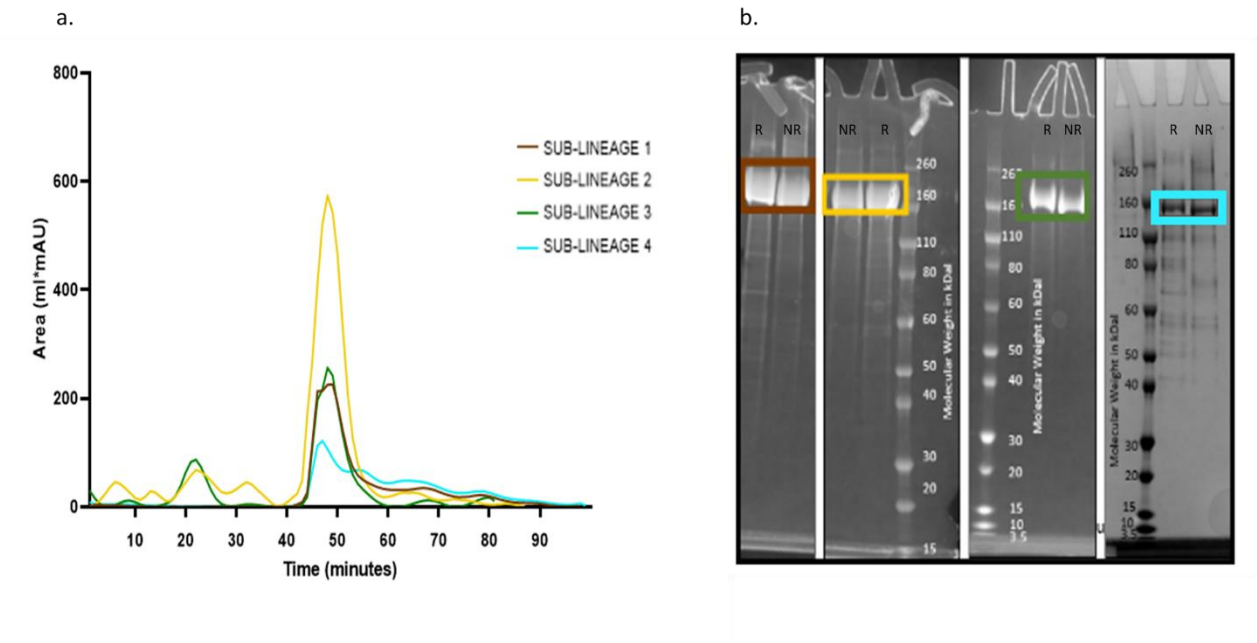

Figure 3.5: Size exclusion chromatograph profiles for purification of sub-lineage 1 – 4 proteins and Reducing and Non-reducing SDS PAGE confirm size of spike protein trimer. (a) Protein trimer eluted from the Nickel sepharose column was separated using the Hiload^{TM} 16/60 Superdex^{TM} 200 column and eluted in 3Mm HEPES buffer. Proteins eluted between 44 – 54 minutes were collected. The X-axis shows the time each fraction was eluted. The Y-axis indicates the concentration of protein that was eluted at each time point. Sub-lineage 1, Sub-lineage 2, Sub-lineage 3 and Sub-lineage 4 spike proteins are represented by brown, yellow, green and cyan colours, respectively. (**b)** Reducing (R) (with 15% β-mercaptoethanol) and non-reducing (NR) SDS PAGE was carried out on purified soluble mutated spike trimers to confirm the size of protein by comparison against a known molecular weight protein marker. Sub-lineage 1 (brown), Sub-lineage 2 (yellow), and Sub-lineage 3 (green)

protein size (160KDa) and purity were confirmed. The Sub-lineage 4 protein (cyan) was observed below the expected 160kDa molecular weight band.

The SARS-CoV-2 spike protomer and each of its composing trimers has a molecular weight of approximately 600kDa and 180 kDa, respectively. Sub-lineage 1, 2, and 3 proteins which were visualized above the 160kDa marker **(Figure 3.5b)**, corresponding to a band at 180kDa and these were used for subsequent ELISA experiments. The purity of Sub-lineage 4 spike proteins was shown to be sub-optimal **(Figure 3.5b)** as multiple protein bands were observed in the non-reducing well indicating that further purification would be required before the protein could be used for ELISA experiments. Therefore, this protein was excluded from subsequent experiments.

3.5 Change in binding between WT and Sub-lineage spike proteins

Polyclonal sera collected during the first wave of infection (where the D614G was the dominant lineage) were used to determine whether sub-lineage spike proteins were recognized by binding antibodies from the first wave. Three-fold serial dilutions were performed starting at a 1:100 plasma dilution **(Figure 3.6)**.

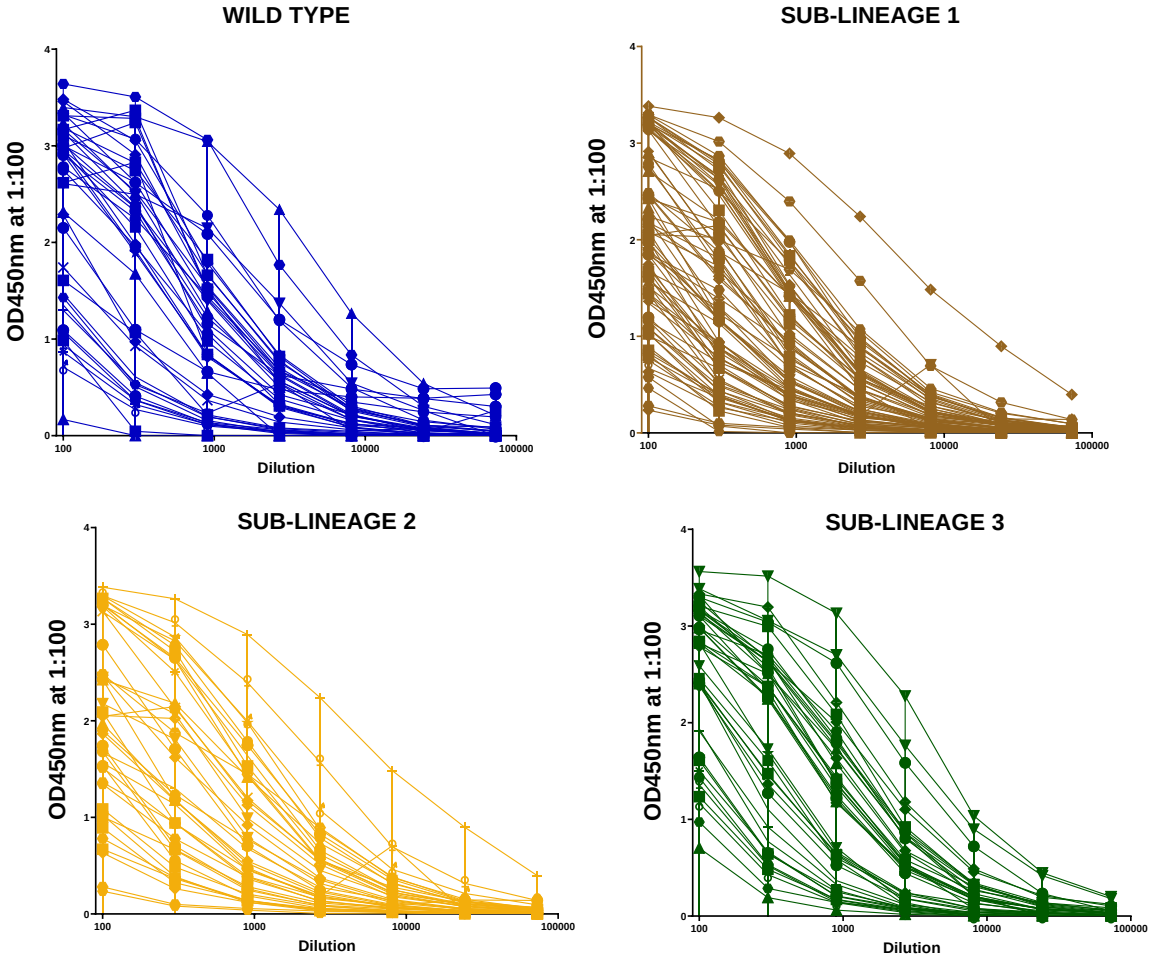

Figure 3.6: ELISA titration graphs for SARS-CoV-2 spike proteins. A graphical representation of ELISA results for convalescent samples by SARS-CoV-2 spike antigen. 3-fold serial dilutions were performed starting at a 1:100 serum plasma dilution.

The optical densities were obtained and GraphPad Prism was used to determine the area under the curve for each sample. The graphs above show that the titration of samples was performed adequately during the study. Of the 42 samples tested, 33% (14/42) of samples show a greater than two-fold reduction in binding Sub-lineage 1 while 28.5% (12/42) of samples showed greater than two-fold reduction in binding Sub-lineage 2 proteins when compared to the WT . A comparison betweenSub-lineage 2 and Sub-lineage 3 proteins showed that 26% (11/42) of samples had a greater than two-fold increase in binding.

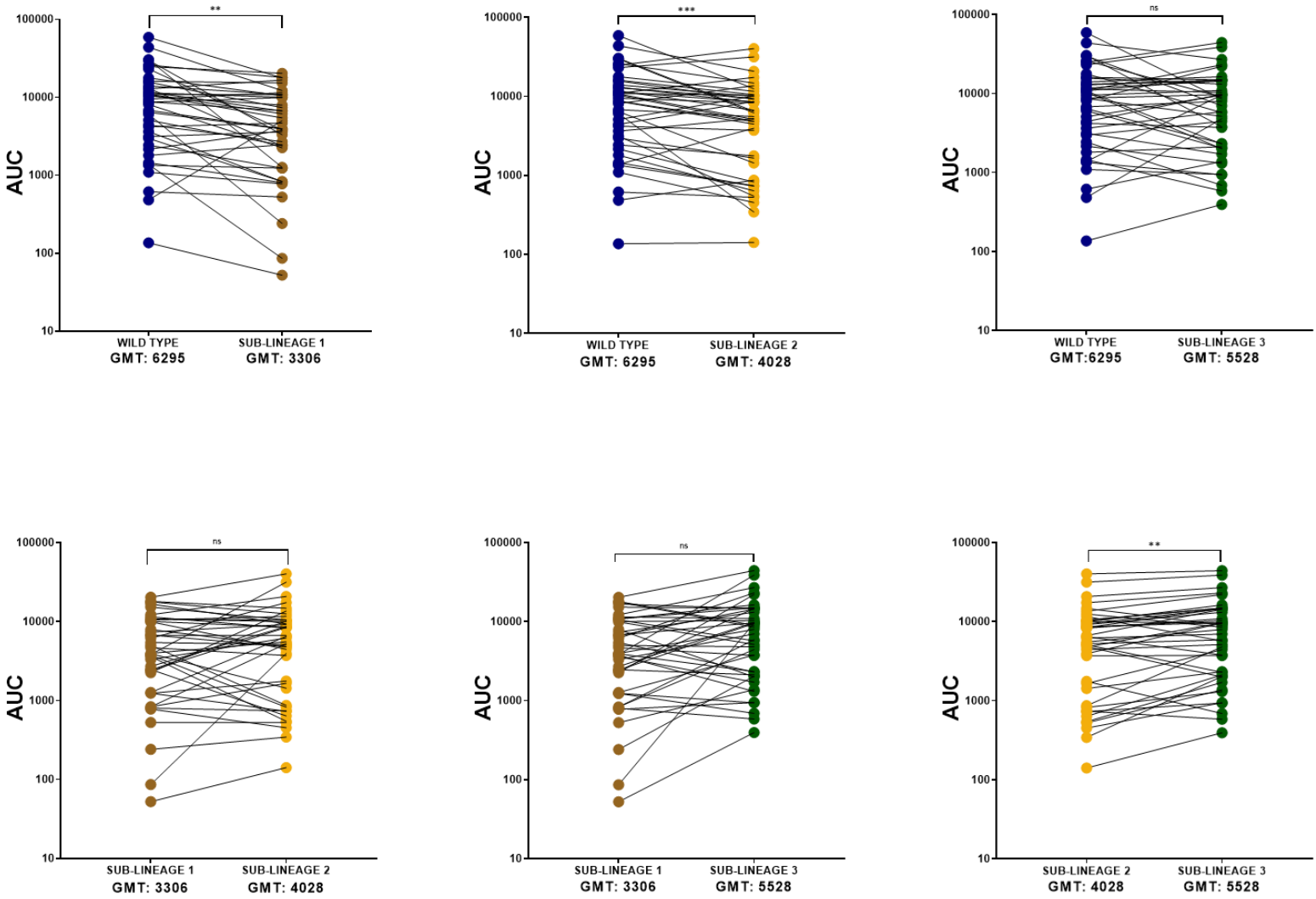

Figure 3.7: Comparison of Area Under the Curve (AUC) between SARS-CoV-2 wild type and sub-lineage spike proteins. A graphical presentation of the change in AUC values between SARS-CoV-2 Wild type, SARS-CoV-2 Sub-lineage 1, SARS-CoV-2 Sub-lineage 2 and SARS-CoV-2 Sub-lineage 3. Geometric mean titres (GMT) for each group are shown. For all experimental tests the statistical significance was calculated using the Friedman's test with Dunn's correction for multiple comparisons. Significant differences between groups where determined where ns $p>0.05$, * $p<0.05$, ** $p<0.01$ and *** $p<0.001$.

Geometric mean titres (GMT) for each group were determined. Statistical analysis using the Friedman's test with Dunn's correction revealed that binding of polyclonal plasma to sub-lineages 1 ($p<0.01$) and sub-lineage 2 ($p<0.001$) spike proteins was significantly reduced compared to the WT. Furthermore, there was a significant ($p<0.01$) increase in binding to Sub-lineage 3 spike protein compared sub-lineage 2 spike protein **(Figure 3.7)**.

3.6 Change in Neutralization Titres

Neutralization assays were used to determine whether SARS-CoV-2 antibodies present in convalescent plasma from the first wave could neutralize the pseudotyped viruses with SARS-CoV-2 sub-lineage spike glycoproteins. Five-fold serial dilutions were performed from a starting dilution of 1:20. Samples were run in duplicate. SARS-CoV-2 strains and ACE2 HEK 293T cells were added and plates were incubated according to protocol. RLUs were obtained and dose response curves were generated for a subset of plasma samples (11/42) representing high, low and medium binding samples **(Figure 3.8)**. The data from these graphs indicate that the plasma samples were able to neutralize the WT and all the sub-lineages pseudoviruses.

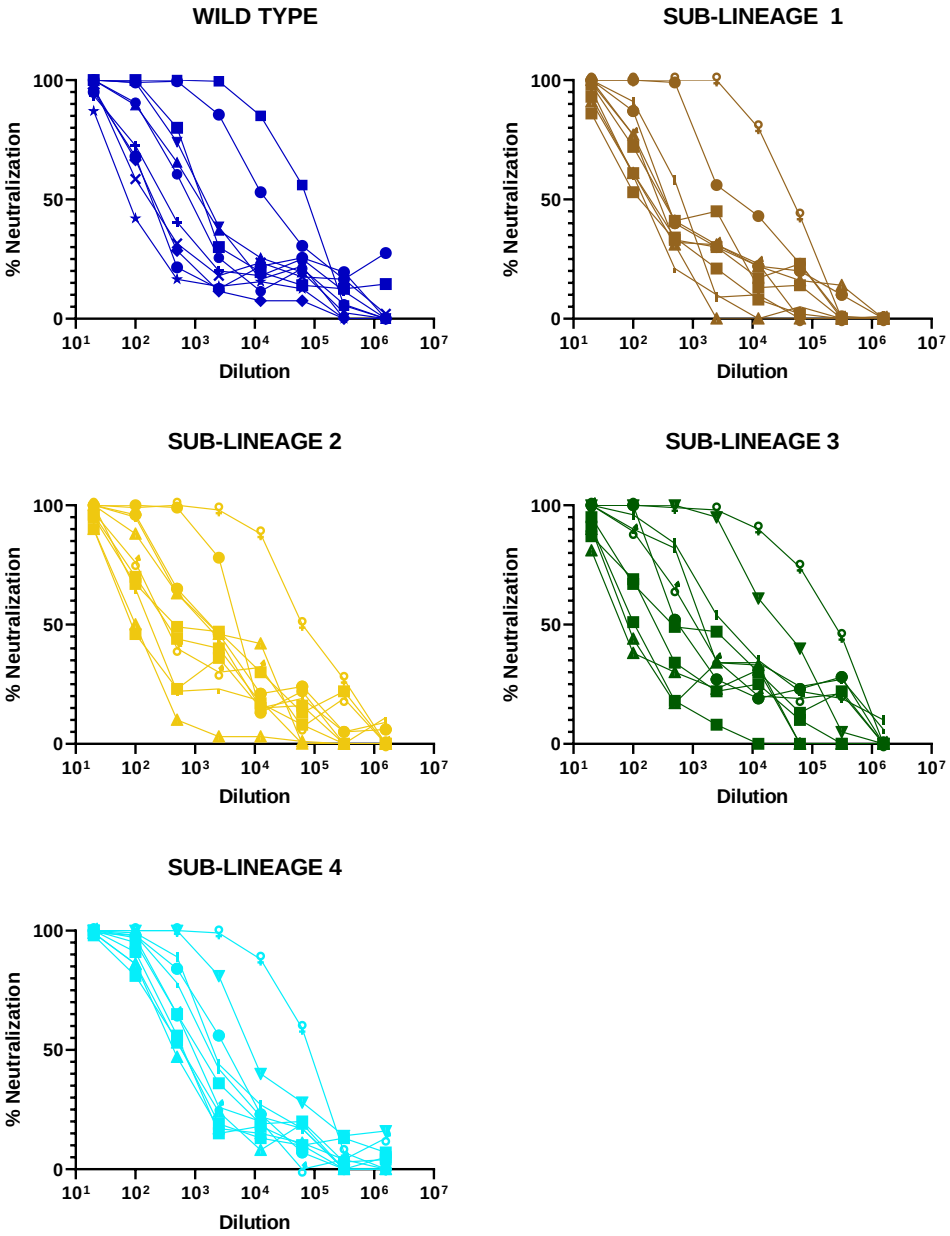

Figure 3.8: Neutralization plot dose-response curves for SARS-CoV-2 wild type and sublineage pseudoviruses. A graphical representation of neutralization results for eleven convalescent samples. Five-fold serial dilutions were performed.

We assessed whether there was any significant change in neutralization sensitivity between the WT and sub-lineage pseudotype viruses. When sub-lineages were compared to the WT pseudovirus, there was no significant change in neutralization sensitivity. The neutralization sensitivity of Sub-lineage pseudovirus to polyclonal plasma was significantly increased compared to the Sub-lineage 1 pseudovirus ($p<0.01$) **(Figure 3.9)**.

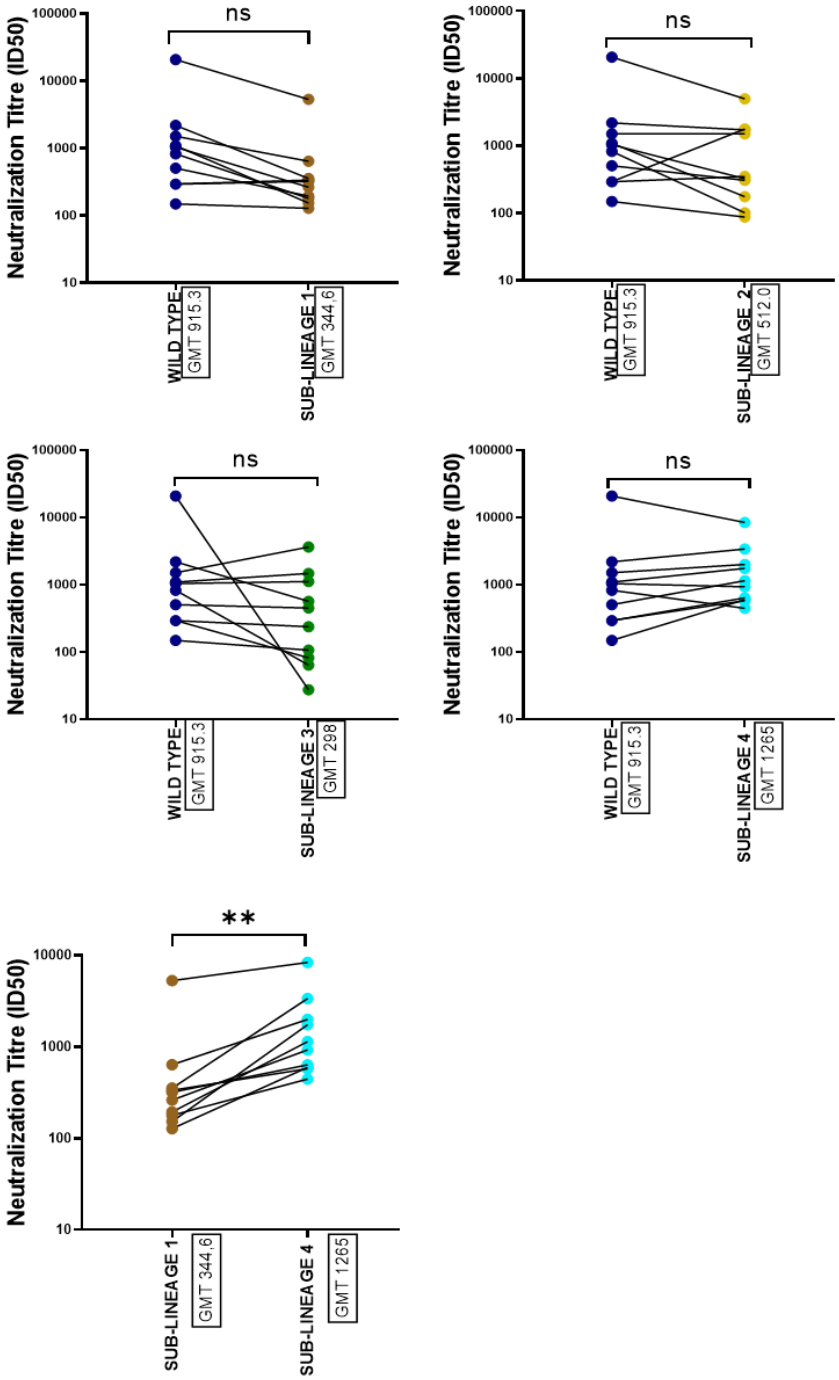

Figure 3.9: Comparison of neutralization titres of SARS-CoV-2 wild type and sub-lineages. A graphical presentation of the change in neutralization titres (ID50) between SARS-CoV-2 Wild type, SARS-CoV-2 Sub-lineage 1, SARS-CoV-2 Sub-lineage 2 and SARS-CoV-2 Sub-lineage 3. Geometric mean titres (GMT) for each group are shown. A significant increase (p-value 0,0069) in neutralization titres was observed between Sub-lineage 1 and Sub-lineage 3. For all experimental tests the statistical significance was calculated using the Friedman's test with Dunn's correction for multiple comparisons. Significant differences between groups where determined where ns $p>0.05$, * $p<0.05$, ** $p<0.01$ and *** $p<0.001$.

Results showed that 63% (7/11) of samples showed a greater than two-fold increase in neutralizing potency from Sub-lineage 1 to Sub-lineage 4 SARS-CoV-2 pseudotype virus **(Figure 3.10)**. Thirty-six percent (4/11) of samples showed a greater than two-fold reduction in neutralization sensitivity to Sub-lineage 2 and Sub-lineage 3spike protein, however, these changes were not statistically significant.

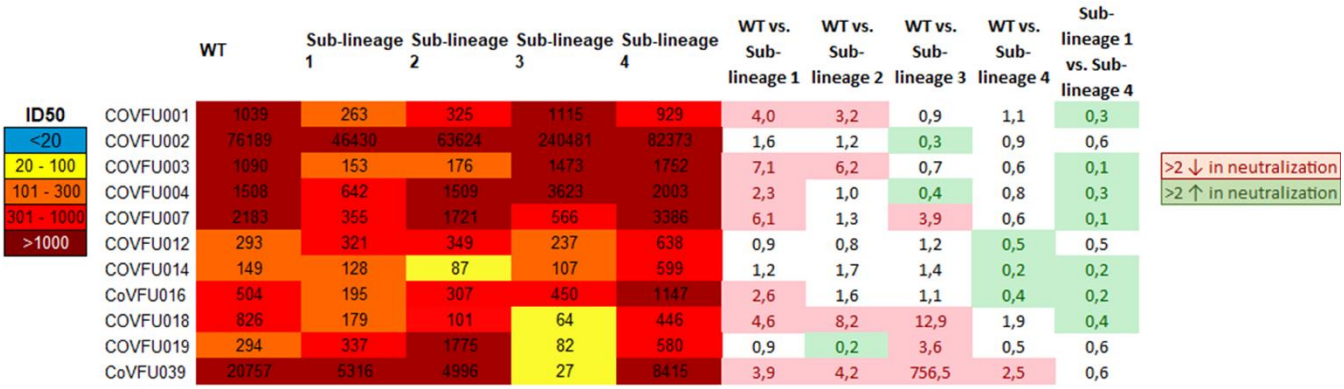

ID50		WT	Sub-lineage 1	Sub-lineage 2	Sub-lineage 3	Sub-lineage 4	WT vs. Sub-lineage 1	WT vs. Sub-lineage 2	WT vs. Sub-lineage 3	WT vs. Sub-lineage 4	Sub-lineage 1 vs. Sub-lineage 4
<20	COVFU001	1039	263	325	1115	929	4,0	3,2	0,9	1,1	0,3
20 - 100	COVFU002	76189	46430	63624	240481	82373	1,6	1,2	0,3	0,9	0,6
101 - 300	COVFU003	1090	153	176	1473	1752	7,1	6,2	0,7	0,6	0,1
301 - 1000	COVFU004	1508	642	1509	3623	2003	2,3	1,0	0,4	0,8	0,3
>1000	COVFU007	2183	355	1721	566	3386	6,1	1,3	3,9	0,6	0,1
	COVFU012	293	321	349	237	638	0,9	0,8	1,2	0,5	0,5
	COVFU014	149	128	87	107	599	1,2	1,7	1,4	0,2	0,2
	CoVFU016	504	195	307	450	1147	2,6	1,6	1,1	0,4	0,2
	COVFU018	826	179	101	64	446	4,6	8,2	12,9	1,9	0,4
	COVFU019	294	337	1775	82	580	0,9	0,2	3,6	0,5	0,6
	CoVFU039	20757	5316	4996	27	8415	3,9	4,2	756,5	2,5	0,6

Figure 3.10: ID50 for each sample against the SARS-CoV-2 wild type and sub-lineages pseudovirus. Change in neutralization sensitivity for each sample. The fold change neutralization sensitivity was determined and samples with a greater than two-fold increase or decrease were highlighted in red and green.

CHAPTER FOUR: DISCUSSION

The continuous evolution of SARS-CoV-2 has resulted in the emergence of VOCs/VOIs with increased transmissibility and reduced immune sensitivity, which has implications for vaccine efforts and re-infections. Monitoring evolutionary changes and their phenotypic characteristics is crucial to support ongoing interventions. Of note are the Delta and Omicron variants. The Delta variant became dominant across the globe due to greater transmissiblility when compared to earlier VOCs including Alpha (105,106). Within VOCs there are sub-lineages with subtle changes to the mutation profile that may have significally different immune escape profiles (107). For example, the Delta variant consists of over 40 sub-lineages (107) including B.1.617.2, AY.1, AY.2, AY.3-AY.12 with defining mutations primarily occurring in the NTD and RBD regions (107,108). The Omicron variant is also characterized by distinct sub-lineages that responded differently to diagnostic tools (109). The differences in non-defining mutations in VOC sublineages may further contribute to differences in viral fitness and immune evasion and therefore, it is crucial to identify and characterize various lineages and sub-lineages that are occurring in different geographic locations. The Omicron variant which was reported in over 34 countries by early December 2021(61) is likely more infectious compared to other VOCs such as the Delta and Beta variants (61). This variant is characterized by multiple mutations within antibody-targetting sites located on the spike protein hence high levels of immune evasion have been reported (46). Nevertheless, the anti-SARS-CoV-2 vaccines still remain effective against this and other variants of concern (50).

From samples collected in December 2020, other researchers from the HTS study identified four sub-lineages of the Beta VOC that contain mutations with potential for immune evasion. The sub-lineages we characterized had mutations in common with those found in the variants that emerged after the second epidemiological wave of infections in South Africa including substitutions located in the NTD and the RBD region. Sub-lineages 1 and 2 showed reduced binding when compared to the WT virus. Reduction in binding of first wave plasma to Sub-lineage 1 spike protein may be a result of the L452R mutation located in the RBD of the spike as shown by results from the *in silico* protein analysis and which is an important immune escape modulator in the Delta and now Omicron variants. The D215G substitution and 241-243 deletion which are associated with decreased binding in the Beta variant likely have contributed to the observed results. Decreases in binding activity - including those directed

towards the NTD - may have implications in the effectiveness of the immune response to SARS-CoV-2 infection as it may be responsible for reduced immune activity such as Fc effector functions (110). Further work may provide insight as to whether mutations in these two sub-lineages have significant impact on Fc-mediated functions. The E484K mutation located in the RBM of the spike protein may explain the greater reduction in binding observed in Sub-lineage 2 as compared to the binding observed in Sub-lineage 1. Despite reduced binding, Sub-lineage 1 and Sub-lineage 2 strains did not show any reduced sensitivity to neutralization. These findings may be due to combined effects of the mutations in the sub-lineages. This may be one reason why these sub-lineages did not significantly increase in frequency so as to alter the epidemiology of SARS-CoV-2 virus in South Africa. Alternatively, the lack of significant changes to neutralization sensitivity for these samples may have resulted from the small number of samples that we used in this study to evaluate neutralization sensitivity.

The Sub-lineage 3 spike protein had a significant increase in binding when compared to Sub-lineage 2 spike protein. The higher binding observed in Sub-lineage 3 spike protein compared to Sub-lineage 2 spike protein may be due to the lack of antibody escape mutations as Sub-lineage 3 only contains the D80A, L452R, Y508H, D614G and A701V mutations while Sub-lineage 2 spike protein differs by having the D215G substitution, the 241-243 deletion, and the E484K mutation in addition to those seen in sub-lineage 3. No significant difference in neutralization sensitivity was observed between the Sub-lineage pseudoviruses and the WT. Furthermore, Sub-lineage 3 pseudovirus and the Sub-lineage 2 pseudovirus did not show significant changes in neutralization sensitivity when compared against each other. This may suggest that the antibodies that were affected by the mutations merely recognized binding epitopes but not neutralizing epitopes. This may suggest that vaccine design should target spike proteins with mutations that are known to affect neutralizating epitopes.

A significant increase in neutralization sensitivity was observed when Sub-lineage 4 pseudovirus neutralization was compared to that of the Sub-lineage 1 pseudovirus. Sub-lineage 4 and Sub-lineage 1 differed by the presence of the deletion at positions 241-243 and the mutation A924T in Sub-lineage 1 and Sub-lineage 4 respectively. The effects of the A924T mutation on neutralization sensitivity have not been characterized, however, the deletion at positions 241-243 in the NTD may contribute to neutralization escape. This NTD deletion has been shown to increase neutralization

resistance, however, in this study no significant change was observed when sub-lineages were compared to the WT pseudovirus. The effects of the deletion at positions 241-243 in Sub-lineage 2 may have been affected by the presence of other mutations within that sub-lineage. Furthermore, these results may be due to the small number of samples that were used by the researcher to assess neutralization.

Structural analysis revealed that amino acid clashes resulting from the L452R mutant spike and the heavy chain of Class II mAb P2B-F26 resulted in the decreased binding affinity of mutant spike to the heavy chain of Class II mAb P2B-F26. The L452R mutation identified by the HTS study in December 2020 has become more dominant since the Delta variant begun circulating in South Africa. The L452R strains may escape neutralization and increase viral infectivity potentially driving infection and re-infection by lineages that carry the L452R mutation. In contrast, the E484K mutation showed a loss of hydrogen bond resulting in a decrease in the binding affinity of mutant spike to the light chain of Class II mAb P2B-F26. In accordance with other studies, findings within this study suggest that the Class II mAbs may exhibit reduced binding and neutralization of viral strains with this mutation.

D614G is present in over 98.5% of circulating SARS-CoV-2 strains and also present in the sub-lineages investigated in this study. This mutation improved the stability of the S1/S2 inter-domain interactions within the spike protein allowing for binding of antibodies when RBD is in the open state (81–83). Furthermore, the D614G change increases the rate of S1/S2 cleavage (84) as well as the number of spike proteins present on the surface of the virion (85,86).

The A701V mutation in the Beta VOC, Sub-lineage 2 and Sub-lineage 3 is located near the furin cleavage site (66). The furin cleavage site is an important determinant of SARS-CoV-2 transmission as mutations occurring within this site potentially increase the cleavage of S1/S2 subunits of the spike protein enhancing viral cell entry (87), however, there is no evidence that the mutation affects neutralization sensitivity of mAbs (66).

One limitation of the study is that we only made use of convalescent plasma from individuals infected with the WT strain from the first wave of infections in South Africa (D614G variant) to determine the changes in binding and neutralization sensitivity of the sub-lineages tested. Future studies on the sensitivity of these and other sub-lineages should include the use of convalescent plasma from currently circulating VOCs to provide more relevant and timely data to the field as antibodies elicited from

other variants may be more cross-reactive compared to the WT and ancestral strains (44). In addition, The impact of mutations that occur outside the spike glycoprotein within these sub-lineages should be investigated for potential effects on the replicative fitness of the virus as this may have contributed to the lack of continued expansion of these lineages.

Our study highlights the need for continuous surveillance of changes to the SARS-CoV-2 spike glycoprotein and the impact these mutations may have on viral transmission, disease severity and immune escape from mAbs used in therapy as well as polyclonal sera elicited by infection and vaccination. Despite reported reduction in vaccine effectiveness against some VOCs, all anti-SARS-CoV-2 vaccines currently in use remain beneficial for immune responses to the virus. SARS-CoV-2 vaccination therefore, remains a key strategy in mitigating the pandemic as vaccines have proved to reduce the burden of disease amid the continued emergence of SARS-CoV-2 variants.

CONCLUSION

This study characterized the antibody responses to four SARS-CoV-2 sub-lineages identified in South Africa. Mutations within these sub-lineages are relevant for immune evasion as they are primarily located in the NTD and the RBD of the spike protein, which are regions where most neutralizing antibody epitopes are located. Several mutations identified in these sub-lineages were defining mutations which are shared by circulating VOC/VOIs. This suggests that the change in the antigenic phenotype of SARS-CoV-2 resulting from viral evolution may drive immune escape. In this study, antibodies showed reduced binding to Sub-lineage 1 and Sub-lineage 2 viruses when compared to the WT virus. Although changes in binding were observed, no significant change was observed in the neutralization sensitivity when the WT was compared to sub-lineage pseudoviruses. The change in binding may be due to mutations that result in the loss of binding epitope recognition, therefore, further research may investigate whether these specific mutations affect Fc receptor binding functions. This study also highlights the importance of genomic surveillance for SARS-CoV-2 coupled with phenotypic investigation of how viral evolution affects immune responses and intervention efforts directed against the pandemic. These findings have implications

for vaccine effectiveness, monoclonal antibody therapies, convalescent plasma and other drug therapies.

REFERENCES

1. Lu S. Timely development of vaccines against SARS-CoV-2. Emerg Microbes Infect. 2020 Jan 1;9(1):542–4.

2. Amanat F, Krammer F. SARS-CoV-2 Vaccines: Status Report. Immunity. 2020 Apr 14;52(4):583–9.

3. WHO Coronavirus (COVID-19) Dashboard [Internet]. [cited 2022 Jan 25]. Available from: https://covid19.who.int

4. Thanh Le T, Andreadakis Z, Kumar A, Gómez Román R, Tollefsen S, Saville M, et al. The COVID-19 vaccine development landscape. Nat Rev Drug Discov. 2020 May;19(5):305–6.

5. Chen L, Xiong J, Bao L, Shi Y. Convalescent plasma as a potential therapy for COVID-19. Lancet Infect Dis. 2020 Apr;20(4):398–400.

6. Bloch EM, Shoham S, Casadevall A, Sachais BS, Shaz B, Winters JL, et al. Deployment of convalescent plasma for the prevention and treatment of COVID-19. J Clin Invest. 2020;130(6):10.

7. Beigel JH, Tomashek KM, Dodd LE, Mehta AK, Zingman BS, Kalil AC, et al. Remdesivir for the Treatment of Covid-19 — Final Report. N Engl J Med. 2020 Nov 5;383(19):1813–26.

8. Szemiel AM, Merits A, Orton RJ, MacLean OA, Pinto RM, Wickenhagen A, et al. In vitro selection of Remdesivir resistance suggests evolutionary predictability of SARS-CoV-2. PLOS Pathog. 2021 Sep 17;17(9):e1009929.

9. Tracking SARS-CoV-2 variants [Internet]. [cited 2021 Sep 3]. Available from: https://www.who.int/emergencies/emergency-health-kits/trauma-emergency-surgery-kit-who-tesk-2019/tracking-SARS-CoV-2-variants

10. Moreira RA, Guzman HV, Boopathi S, Baker JL, Poma AB. Characterization of Structural and Energetic Differences between Conformations of the SARS-CoV-2 Spike Protein. Materials. 2020 Jan;13(23):5362.

11. Mariano G, Farthing RJ, Lale-Farjat SLM, Bergeron JRC. Structural Characterization of SARS-CoV-2: Where We Are, and Where We Need to Be. Front Mol Biosci. 2020;7:344.

12. Naqvi AAT, Fatima K, Mohammad T, Fatima U, Singh IK, Singh A, et al. Insights into SARS-CoV-2 genome, structure, evolution, pathogenesis and therapies: Structural genomics approach. Biochim Biophys Acta BBA - Mol Basis Dis. 2020 Oct 1;1866(10):165878.

13. Eakachai P, Ketloi C, Palaga T. Immune responses in COVID-19 and potential vaccines: Lessons learned from SARS and MERS epidemic. Asian Pac J Allergy Immunol. 2020;38:1–9.

14. Helmy YA, Fawzy M, Elaswad A, Sobieh A, Kenney SP, Shehata AA. The COVID-19 Pandemic: A Comprehensive Review of Taxonomy, Genetics, Epidemiology, Diagnosis, Treatment, and Control. J Clin Med. 2020 Apr 24;9(4):1225.

15. Gur M, Taka E, Yilmaz SZ, Kilinc C, Aktas U, Golcuk M. Conformational transition of SARS-CoV-2 spike glycoprotein between its closed and open states. J Chem Phys. 2020 Aug 21;153(7):075101.

16. Peacock TP, Goldhill DH, Zhou J, Baillon L, Frise R, Swann OC, et al. The furin cleavage site in the SARS-CoV-2 spike protein is required for transmission in ferrets. Nat Microbiol. 2021 Jul;6(7):899–909.

17. Xu C, Wang Y, Liu C, Zhang C, Han W, Hong X, et al. Conformational dynamics of SARS-CoV-2 trimeric spike glycoprotein in complex with receptor ACE2 revealed by cryo-EM. Sci Adv. 7(1):eabe5575.

18. Chen Y, Tong X, Li Y, Gu B, Yan J, Liu Y, et al. A comprehensive, longitudinal analysis of humoral responses specific to four recombinant antigens of SARS-CoV-2 in severe and non-severe COVID-19 patients. PLOS Pathog. 2020 Sep 10;16(9):e1008796.

19. Sterlin D, Mathian A, Miyara M, Mohr A, Anna F, Claër L, et al. IgA dominates the early neutralizing antibody response to SARS-CoV-2. Sci Transl Med. 2021 Jan 20;13(577):eabd2223.

20. Glück V, Grobecker S, Tydykov L, Salzberger B, Glück T, Weidlich T, et al. SARS-CoV-2-directed antibodies persist for more than six months in a cohort with mild to moderate COVID-19. Infection. 2021 Aug;49(4):739–46.

21. Fraley E, LeMaster C, Geanes E, Banerjee D, Khanal S, Grundberg E, et al. Humoral immune responses during SARS-CoV-2 mRNA vaccine administration in seropositive and seronegative individuals. BMC Med. 2021 Jul 26;19(1):169.

22. Atyeo C, Slein MD, Fischinger S, Burke J, Schäfer A, Leist SR, et al. Dissecting strategies to tune the therapeutic potential of SARS-CoV-2–specific monoclonal antibody CR3022. JCI Insight. 6(1):e143129.

23. Ho M. Perspectives on the development of neutralizing antibodies against SARS-CoV-2. Antib Ther. 2020 Apr;3(2):109–14.

24. Brochot E, Demey B, Touzé A, Belouzard S, Dubuisson J, Schmit JL, et al. Anti-spike, Anti-nucleocapsid and Neutralizing Antibodies in SARS-CoV-2 Inpatients and Asymptomatic Individuals. Front Microbiol. 2020 Oct 19;11:584251.

25. Barnes CO, Jette CA, Abernathy ME, Dam KMA, Esswein SR, Gristick HB, et al. SARS-CoV-2 neutralizing antibody structures inform therapeutic strategies. Nature. 2020 Dec 24;588(7839):682–7.

26. Wibmer CK, Ayres F, Hermanus T, Madzivhandila M, Kgagudi P, Oosthuysen B, et al. SARS-CoV-2 501Y.V2 escapes neutralization by South African COVID-19 donor plasma. Nat Med. 2021 Apr;27(4):622–5.

27. Greaney AJ, Starr TN, Barnes CO, Weisblum Y, Schmidt F, Caskey M, et al. Mapping mutations to the SARS-CoV-2 RBD that escape binding by different classes of antibodies. Nat Commun. 2021 Jul 7;12(1):4196.

28. Chi X, Yan R, Zhang J, Zhang G, Zhang Y, Hao M, et al. A neutralizing human antibody binds to the N-terminal domain of the Spike protein of SARS-CoV-2. Science. 2020 Aug 7;369(6504):650–5.

29. Suryadevara N, Shrihari S, Gilchuk P, VanBlargan LA, Binshtein E, Zost SJ, et al. Neutralizing and protective human monoclonal antibodies recognizing the N-terminal domain of the SARS-CoV-2 spike protein. Cell. 2021 Apr 29;184(9):2316-2331.e15.

30. McCallum M, De Marco A, Lempp FA, Tortorici MA, Pinto D, Walls AC, et al. N-terminal domain antigenic mapping reveals a site of vulnerability for SARS-CoV-2. Cell. 2021 Apr 29;184(9):2332-2347.e16.

31. Lok SM. An NTD supersite of attack. Cell Host Microbe. 2021 May 12;29(5):744–6.

32. Shah P, Canziani GA, Carter EP, Chaiken I. The Case for S2: The Potential Benefits of the S2 Subunit of the SARS-CoV-2 Spike Protein as an Immunogen in Fighting the COVID-19 Pandemic. Front Immunol. 2021;12:508.

33. Heffron AS, McIlwain SJ, Amjadi MF, Baker DA, Khullar S, Armbrust T, et al. The landscape of antibody binding in SARS-CoV-2 infection. Alter G, editor. PLOS Biol. 2021 Jun 18;19(6):e3001265.

34. Brüssow H. COVID-19: emergence and mutational diversification of SARS-CoV-2. Microb Biotechnol. 2021 Mar 22;14(3):756–68.

35. Rochman ND, Wolf YI, Faure G, Mutz P, Zhang F, Koonin EV. Ongoing global and regional adaptive evolution of SARS-CoV-2. Proc Natl Acad Sci. 2021 Jul 20;118(29):e2104241118.

36. Jackson CB, Zhang L, Farzan M, Choe H. Functional importance of the D614G mutation in the SARS-CoV-2 spike protein. Biochem Biophys Res Commun. 2021 Jan 29;538:108–15.

37. Thomson EC, Rosen LE, Shepherd JG, Spreafico R, da Silva Filipe A, Wojcechowskyj JA, et al. Circulating SARS-CoV-2 spike N439K variants maintain fitness while evading antibody-mediated immunity. Cell. 2021 Mar 4;184(5):1171-1187.e20.

38. Farkas C, Mella A, Haigh JJ. Large-scale population analysis of SARS-CoV-2 whole genome sequences reveals host-mediated viral evolution with emergence of mutations in the viral Spike protein associated with elevated mortality rates

[Internet]. 2020 Oct [cited 2021 Nov 25] p. 2020.10.23.20218511. Available from: https://www.medrxiv.org/content/10.1101/2020.10.23.20218511v1

39. Tegally H, Wilkinson E, Lessells RJ, Giandhari J, Pillay S, Msomi N, et al. Sixteen novel lineages of SARS-CoV-2 in South Africa. Nat Med. 2021 Mar;27(3):440–6.

40. Tracking SARS-CoV-2 variants [Internet]. [cited 2022 Jan 25]. Available from: https://www.who.int/emergencies/what-we-do/tracking-SARS-CoV-2-variants

41. GISAID - Initiative [Internet]. 2020 [cited 2020 Oct 5]. Available from: https://www.gisaid.org/

42. Tao K, Tzou PL, Nouhin J, Gupta RK, de Oliveira T, Kosakovsky Pond SL, et al. The biological and clinical significance of emerging SARS-CoV-2 variants. Nat Rev Genet. 2021 Sep 17;1–17.

43. Planas D, Veyer D, Baidaliuk A, Staropoli I, Guivel-Benhassine F, Rajah MM, et al. Reduced sensitivity of SARS-CoV-2 variant Delta to antibody neutralization. Nature. 2021 Aug;596(7871):276–80.

44. Moyo-Gwete T, Madzivhandila M, Makhado Z, Ayres F, Mhlanga D, Oosthuysen B, et al. SARS-CoV-2 501Y.V2 (B.1.351) elicits cross-reactive neutralizing antibodies. BioRxiv Prepr Serv Biol. 2021 Mar 11;2021.03.06.434193.

45. Scheepers C, Everatt J, Amoako D, Tegally H, Wibmer CK, Mnguni A, et al. Emergence and phenotypic characterization of C.1.2, a globally detected lineage that rapidly accumulated mutations of concer [Internet]. 2021 [cited 2021 Dec 27]. Available from: https://europepmc.org/article/PPR/PPR387142

46. Kannan SR, Spratt AN, Sharma K, Chand HS, Byrareddy SN, Singh K. Omicron SARS-CoV-2 variant: Unique features and their impact on pre-existing antibodies. J Autoimmun. 2022 Jan 1;126:102779.

47. Wu L, Zhou L, Mo M, Li Y, Han J, Li J, et al. The effect of the multiple mutations in Omicron RBD on its binding to human ACE2 receptor and immune evasion: an investigation of molecular dynamics simulations. 2021 Dec 7 [cited 2021 Dec 19]; Available from: https://chemrxiv.org/engage/chemrxiv/article-details/61acb409bc299c44248a2b12

48. Viana R, Moyo S, Amoako DG, Tegally H, Scheepers C, Althaus CL, et al. Rapid epidemic expansion of the SARS-CoV-2 Omicron variant in southern Africa. Nature. 2022 Jan 7;1–10.

49. Choi A, Koch M, Wu K, Chu L, Ma L, Hill A, et al. Safety and immunogenicity of SARS-CoV-2 variant mRNA vaccine boosters in healthy adults: an interim analysis. Nat Med. 2021 Nov;27(11):2025–31.

50. Cele S, Jackson L, Khoury DS, Khan K, Moyo-Gwete T, Tegally H, et al. Omicron extensively but incompletely escapes Pfizer BNT162b2 neutralization. Nature. 2021 Dec 23;d41586-021-03824–5.

51. Supasa P, Zhou D, Dejnirattisai W, Liu C, Mentzer AJ, Ginn HM, et al. Reduced neutralization of SARS-CoV-2 B.1.1.7 variant by convalescent and vaccine sera. Cell. 2021 Apr 15;184(8):2201-2211.e7.

52. Gidari A, Sabbatini S, Bastianelli S, Pierucci S, Busti C, Monari C, et al. Cross-neutralization of SARS-CoV-2 B.1.1.7 and P.1 variants in vaccinated, convalescent and P.1 infected. J Infect. 2021 Oct 1;83(4):467–72.

53. Zhou D, Dejnirattisai W, Supasa P, Liu C, Mentzer AJ, Ginn HM, et al. Evidence of escape of SARS-CoV-2 variant B.1.351 from natural and vaccine-induced sera. Cell. 2021 Apr 29;184(9):2348-2361.e6.

54. Ren W, Ju X, Gong M, Lan J, Yu Y, Long Q, et al. Characterization of SARS-CoV-2 variants B.1.617.1 (Kappa), B.1.617.2 (Delta) and B.1.618 on cell entry, host range, and sensitivity to convalescent plasma and ACE2 decoy receptor [Internet]. 2021 Sep [cited 2021 Sep 27] p. 2021.09.03.458829. Available from: https://www.biorxiv.org/content/10.1101/2021.09.03.458829v1

55. Zhou H, Dcosta BM, Samanovic MI, Mulligan MJ, Landau NR, Tada T. B.1.526 SARS-CoV-2 variants identified in New York City are neutralized by vaccine-elicited and therapeutic monoclonal antibodies [Internet]. Immunology; 2021 Mar [cited 2021 Mar 29]. Available from: http://biorxiv.org/lookup/doi/10.1101/2021.03.24.436620

56. Tada T, Zhou H, Dcosta BM, Samanovic MI, Mulligan MJ, Landau NR. SARS-CoV-2 Lambda Variant Remains Susceptible to Neutralization by mRNA Vaccine-elicited Antibodies and Convalescent Serum [Internet]. 2021 Jul [cited 2021 Oct 14] p. 2021.07.02.450959. Available from: https://www.biorxiv.org/content/10.1101/2021.07.02.450959v1

57. Uriu K, Kimura I, Shirakawa K, Takaori-Kondo A, Nakada T aki, Kaneda A, et al. Ineffective neutralization of the SARS-CoV-2 Mu variant by convalescent and vaccine sera [Internet]. 2021 Sep [cited 2021 Oct 25] p. 2021.09.06.459005. Available from: https://www.biorxiv.org/content/10.1101/2021.09.06.459005v1

58. Dicken SJ, Murray MJ, Thorne LG, Reuschl AK, Forrest C, Ganeshalingham M, et al. Characterisation of B.1.1.7 and Pangolin coronavirus spike provides insights on the evolutionary trajectory of SARS-CoV-2. bioRxiv. 2021 Mar 22;2021.03.22.436468.

59. Faria NR, Mellan TA, Whittaker C, Claro IM, Candido D da S, Mishra S, et al. Genomics and epidemiology of the P.1 SARS-CoV-2 lineage in Manaus, Brazil. Science. 2021 May 21;372(6544):815–21.

60. Dhar MS, Marwal R, Radhakrishnan V, Ponnusamy K, Jolly B, Bhoyar RC, et al. Genomic characterization and Epidemiology of an emerging SARS-CoV-2 variant in Delhi, India [Internet]. Epidemiology; 2021 Jun [cited 2021 Sep 10]. Available from: http://medrxiv.org/lookup/doi/10.1101/2021.06.02.21258076

61. He X, Hong W, Pan X, Lu G, Wei X. SARS-CoV-2 Omicron variant: Characteristics and prevention. MedComm. 2021;2(4):838–45.

62. Garcia-Beltran WF, St. Denis KJ, Hoelzemer A, Lam EC, Nitido AD, Sheehan ML, et al. mRNA-based COVID-19 vaccine boosters induce neutralizing immunity against SARS-CoV-2 Omicron variant. Cell [Internet]. 2022 Jan 6 [cited 2022 Jan 24]; Available from: https://www.sciencedirect.com/science/article/pii/S0092867421014963

63. Ozer EA, Simons LM, Adewumi OM, Fowotade AA, Omoruyi EC, Adeniji JA, et al. High prevalence of SARS-CoV-2 B.1.1.7 (UK variant) and the novel B.1.5.2.5 lineage in Oyo State, Nigeria [Internet]. 2021 Apr [cited 2021 Sep 10] p. 2021.04.09.21255206. Available from: https://www.medrxiv.org/content/10.1101/2021.04.09.21255206v1

64. Annavajhala MK, Mohri H, Wang P, Nair M, Zucker JE, Sheng Z, et al. Emergence and Expansion of the SARS-CoV-2 Variant B.1.526 Identified in New York. medRxiv. 2021 Aug 4;2021.02.23.21252259.

65. Ferreira I, Datir R, Papa G, Kemp S, Meng B, Rakshit P, et al. SARS-CoV-2 B.1.617 emergence and sensitivity to vaccine-elicited antibodies [Internet]. 2021 May [cited 2021 Sep 10] p. 2021.05.08.443253. Available from: https://www.biorxiv.org/content/10.1101/2021.05.08.443253v1

66. Romero PE, Dávila-Barclay A, Salvatierra G, González L, Cuicapuza D, Solís L, et al. The Emergence of Sars-CoV-2 Variant Lambda (C.37) in South America. Microbiol Spectr [Internet]. 2021 Oct 27 [cited 2022 Jan 11]; Available from: https://journals.asm.org/doi/abs/10.1128/Spectrum.00789-21

67. Laiton-Donato K, Franco-Muñoz C, Álvarez-Díaz DA, Ruiz-Moreno HA, Usme-Ciro JA, Prada DA, et al. Characterization of the emerging B.1.621 variant of interest of SARS-CoV-2 [Internet]. 2021 May [cited 2021 Sep 10] p. 2021.05.08.21256619. Available from: https://www.medrxiv.org/content/10.1101/2021.05.08.21256619v1

68. Shen X, Tang H, McDanal C, Wagh K, Fischer W, Theiler J, et al. SARS-CoV-2 variant B.1.1.7 is susceptible to neutralizing antibodies elicited by ancestral spike vaccines. Cell Host Microbe. 2021 Apr 14;29(4):529-539.e3.

69. Mohammadi M, Shayestehpour M, Mirzaei H. The impact of spike mutated variants of SARS-CoV2 [Alpha, Beta, Gamma, Delta, and Lambda] on the efficacy of subunit recombinant vaccines. Braz J Infect Dis. 2021 Jul 1;25(4):101606.

70. Hoffmann M, Arora P, Groß R, Seidel A, Hörnich B, Hahn A, et al. SARS-CoV-2 variants B.1.351 and B.1.1.248: Escape from therapeutic antibodies and antibodies induced by infection and vaccination [Internet]. 2021 Feb [cited 2021 Sep 27] p. 2021.02.11.430787. Available from: https://www.biorxiv.org/content/10.1101/2021.02.11.430787v1

71. Wang P, Nair MS, Liu L, Iketani S, Luo Y, Guo Y, et al. Antibody resistance of SARS-CoV-2 variants B.1.351 and B.1.1.7. Nature. 2021 May 6;593(7857):130–5.

72. Davis C, Logan N, Tyson G, Orton R, Harvey WT, Perkins JS, et al. Reduced neutralisation of the Delta (B.1.617.2) SARS-CoV-2 variant of concern following vaccination. PLOS Pathog. 2021 Dec 2;17(12):e1010022.

73. Wall EC, Wu M, Harvey R, Kelly G, Warchal S, Sawyer C, et al. Neutralising antibody activity against SARS-CoV-2 VOCs B.1.617.2 and B.1.351 by BNT162b2 vaccination. The Lancet. 2021 Jun;397(10292):2331–3.

74. Fischer W, Giorgi EE, Chakraborty S, Nguyen K, Bhattacharya T, Theiler J, et al. HIV-1 and SARS-CoV-2: Patterns in the evolution of two pandemic pathogens. Cell Host Microbe. 2021 Jul 14;29(7):1093–110.

75. Harvey WT, Carabelli AM, Jackson B, Gupta RK, Thomson EC, Harrison EM, et al. SARS-CoV-2 variants, spike mutations and immune escape. Nat Rev Microbiol. 2021 Jul;19(7):409–24.

76. Tatsi EB, Filippatos F, Michos A. SARS-CoV-2 variants and effectiveness of vaccines: a review of current evidence. Epidemiol Infect [Internet]. 2021 ed [cited 2021 Nov 29];149. Available from: https://www.cambridge.org/core/journals/epidemiology-and-infection/article/sarscov2-variants-and-effectiveness-of-vaccines-a-review-of-current-evidence/39243FCC3CED73D5F1D94E497F8823D3

77. Ali F, Kasry A, Amin M. The new SARS-CoV-2 strain shows a stronger binding affinity to ACE2 due to N501Y mutant. Med Drug Discov. 2021 Jun 1;10:100086.

78. Shi R, Shan C, Duan X, Chen Z, Liu P, Song J, et al. A human neutralizing antibody targets the receptor-binding site of SARS-CoV-2. Nature. 2020 Aug;584(7819):120–4.

79. Luan B, Huynh T. Insights into SARS-CoV-2's Mutations for Evading Human Antibodies: Sacrifice and Survival. J Med Chem [Internet]. 2021 Apr 9 [cited 2022 Jan 11]; Available from: https://doi.org/10.1021/acs.jmedchem.1c00311

80. Jangra S, Ye C, Rathnasinghe R, Stadlbauer D, Group P study, Krammer F, et al. The E484K mutation in the SARS-CoV-2 spike protein reduces but does not abolish neutralizing activity of human convalescent and post-vaccination sera [Internet]. 2021 Jan [cited 2021 Sep 3] p. 2021.01.26.21250543. Available from: https://www.medrxiv.org/content/10.1101/2021.01.26.21250543v1

81. Nelson G, Buzko O, Spilman P, Niazi K, Rabizadeh S, Soon-Shiong P. Molecular dynamic simulation reveals E484K mutation enhances spike RBD-ACE2 affinity and the combination of E484K, K417N and N501Y mutations (501Y.V2 variant) induces conformational change greater than N501Y mutant alone, potentially resulting in an escape mutant [Internet]. 2021 Jan [cited 2021 Sep 27] p. 2021.01.13.426558. Available from: https://www.biorxiv.org/content/10.1101/2021.01.13.426558v1

82. Deng X, Garcia-Knight MA, Khalid MM, Servellita V, Wang C, Morris MK, et al. Transmission, infectivity, and neutralization of a spike L452R SARS-CoV-2 variant. Cell. 2021 Jun 24;184(13):3426-3437.e8.

83. Deng X, Garcia-Knight MA, Khalid MM, Servellita V, Wang C, Morris MK, et al. Transmission, infectivity, and antibody neutralization of an emerging SARS-CoV-2 variant in California carrying a L452R spike protein mutation [Internet]. 2021 Mar [cited 2021 Sep 3] p. 2021.03.07.21252647. Available from: https://www.medrxiv.org/content/10.1101/2021.03.07.21252647v1

84. Lubinski B, Tang T, Daniel S, Jaimes JA, Whittaker GR. Functional evaluation of proteolytic activation for the SARS-CoV-2 variant B.1.1.7: role of the P681H mutation. bioRxiv. 2021 Apr 8;2021.04.06.438731.

85. Mlcochova P, Kemp SA, Dhar MS, Papa G, Meng B, Ferreira IATM, et al. SARS-CoV-2 B.1.617.2 Delta variant replication and immune evasion. Nature. 2021 Nov;599(7883):114–9.

86. WHO lists additional COVID-19 vaccine for emergency use and issues interim policy recommendations [Internet]. [cited 2021 Aug 31]. Available from: https://www.who.int/news/item/07-05-2021-who-lists-additional-covid-19-vaccine-for-emergency-use-and-issues-interim-policy-recommendations

87. The COVID-19 vaccine race [Internet]. [cited 2021 Aug 31]. Available from: https://www.gavi.org/vaccineswork/covid-19-vaccine-race

88. Fowlkes A, Gaglani M, Groover K, Thiese MS, Tyner H, Ellingson K. Effectiveness of COVID-19 Vaccines in Preventing SARS-CoV-2 Infection Among Frontline Workers Before and During B.1.617.2 (Delta) Variant Predominance — Eight U.S. Locations, December 2020–August 2021. Morb Mortal Wkly Rep. 2021 Aug 27;70(34):1167–9.

89. Pilishvili T, Gierke R, Fleming-Dutra KE, Farrar JL, Mohr NM, Talan DA, et al. Effectiveness of mRNA Covid-19 Vaccine among U.S. Health Care Personnel. N Engl J Med. 2021 Sep 22;0(0):null.

90. Abu-Raddad LJ, Chemaitelly H, Butt AA. Effectiveness of the BNT162b2 Covid-19 Vaccine against the B.1.1.7 and B.1.351 Variants. N Engl J Med. 2021 Jul 8;385(2):187–9.

91. Tang P, Hasan MR, Chemaitelly H, Yassine HM, Benslimane FM, Al Khatib HA, et al. BNT162b2 and mRNA-1273 COVID-19 vaccine effectiveness against the SARS-CoV-2 Delta variant in Qatar. Nat Med. 2021 Dec;27(12):2136–43.

92. Gómez CE, Perdiguero B, Esteban M. Emerging SARS-CoV-2 Variants and Impact in Global Vaccination Programs against SARS-CoV-2/COVID-19. Vaccines. 2021 Mar;9(3):243.

93. Charmet T, Schaeffer L, Grant R, Galmiche S, Chény O, Von Platen C, et al. Impact of original, B.1.1.7, and B.1.351/P.1 SARS-CoV-2 lineages on vaccine effectiveness of two doses of COVID-19 mRNA vaccines: Results from a

nationwide case-control study in France. Lancet Reg Health - Eur. 2021 Sep;8:100171.

94. Thompson MG, Burgess JL, Naleway AL, Tyner HL, Yoon SK, Meece J, et al. Interim Estimates of Vaccine Effectiveness of BNT162b2 and mRNA-1273 COVID-19 Vaccines in Preventing SARS-CoV-2 Infection Among Health Care Personnel, First Responders, and Other Essential and Frontline Workers — Eight U.S. Locations, December 2020–March 2021. MMWR Morb Mortal Wkly Rep. 2021 Apr 2;70(13):495–500.

95. Nasreen S, He S, Chung H, Brown KA, Gubbay JB, Buchan SA, et al. Effectiveness of COVID-19 vaccines against variants of concern, Canada [Internet]. 2021 Jul [cited 2021 Sep 29] p. 2021.06.28.21259420. Available from: https://www.medrxiv.org/content/10.1101/2021.06.28.21259420v1

96. Sheikh A, McMenamin J, Taylor B, Robertson C. SARS-CoV-2 Delta VOC in Scotland: demographics, risk of hospital admission, and vaccine effectiveness. The Lancet. 2021 Jun 26;397(10293):2461–2.

97. Thiruvengadam R, Awasthi A, Medigeshi G, Bhattacharya S, Mani S, Sivasubbu S, et al. Cellular Immune Responses are Preserved and May Contribute to Chadox1 ChAdOx1 nCoV-19 Vaccine Effectiveness Against Infection Due to SARS-CoV-2 B·1·617·2 Delta Variant Despite Reduced Virus Neutralisation [Internet]. Rochester, NY: Social Science Research Network; 2021 Jul [cited 2021 Sep 29]. Report No.: ID 3884946. Available from: https://papers.ssrn.com/abstract=3884946

98. Barlow RS, Jian K, Larson L. Effectiveness of COVID-19 Vaccines Against SARS-CoV-2 Infection During a Delta Variant Epidemic Surge in Multnomah County, Oregon, July 2021 [Internet]. 2021 Sep [cited 2021 Sep 29] p. 2021.08.30.21262446. Available from: https://www.medrxiv.org/content/10.1101/2021.08.30.21262446v1

99. Chemaitelly H, Yassine HM, Benslimane FM, Al Khatib HA, Tang P, Hasan MR, et al. mRNA-1273 COVID-19 vaccine effectiveness against the B.1.1.7 and B.1.351 variants and severe COVID-19 disease in Qatar. Nat Med. 2021 Sep;27(9):1614–21.

100. Li XN, Huang Y, Wang W, Jing QL, Zhang CH, Qin PZ, et al. Effectiveness of inactivated SARS-CoV-2 vaccines against the Delta variant infection in Guangzhou: a test-negative case–control real-world study. Emerg Microbes Infect. 2021 Jan 1;10(1):1751–9.

101. Hsieh CL, Goldsmith JA, Schaub JM, DiVenere AM, Kuo HC, Javanmardi K, et al. Structure-based design of prefusion-stabilized SARS-CoV-2 spikes. Science. 2020 Sep 18;369(6510):1501–5.

102. Longo PA, Kavran JM, Kim MS, Leahy DJ. Transient Mammalian Cell Transfection with Polyethylenimine (PEI). Methods Enzymol. 2013;529:227–40.

103. Amanat F, Stadlbauer D, Strohmeier S, Nguyen THO, Chromikova V, McMahon M, et al. A serological assay to detect SARS-CoV-2 seroconversion in humans. Nat Med. 2020 Jul;26(7):1033–6.

104. Motozono C, Toyoda M, Zahradnik J, Saito A, Nasser H, Tan TS, et al. SARS-CoV-2 spike L452R variant evades cellular immunity and increases infectivity. Cell Host Microbe. 2021 Jul 14;29(7):1124-1136.e11.

105. Kannan SR, Spratt AN, Cohen AR, Naqvi SH, Chand HS, Quinn TP, et al. Evolutionary analysis of the Delta and Delta Plus variants of the SARS-CoV-2 viruses. J Autoimmun. 2021 Nov 1;124:102715.

106. Ju B, Zhang Q, Ge J, Wang R, Sun J, Ge X, et al. Human neutralizing antibodies elicited by SARS-CoV-2 infection. Nature. 2020 Aug;584(7819):115–9.

107. Baj A, Novazzi F, Drago Ferrante F, Genoni A, Tettamanzi E, Catanoso G, et al. Spike protein evolution in the SARS-CoV-2 Delta variant of concern: a case series from Northern Lombardy. Emerg Microbes Infect. 2021 Jan 1;10(1):2010–5.

108. Shen L, Triche TJ, Bard JD, Biegel JA, Judkins AR, Gai X. Spike Protein NTD mutation G142D in SARS-CoV-2 Delta VOC lineages is associated with frequent back mutations, increased viral loads, and immune evasion [Internet]. Infectious Diseases (except HIV/AIDS); 2021 Sep [cited 2021 Nov 19]. Available from: http://medrxiv.org/lookup/doi/10.1101/2021.09.12.21263475

109. Christensen PA, Olsen RJ, Long SW, Snehal R, Davis JJ, Saavedra MO, et al. Signals of significantly increased vaccine breakthrough, decreased hospitalization rates, and less severe disease in patients with COVID-19 caused by the Omicron variant of SARS-CoV-2 in Houston, Texas [Internet]. medRxiv; 2022 [cited 2022 Jan 24]. p. 2021.12.30.21268560. Available from: https://www.medrxiv.org/content/10.1101/2021.12.30.21268560v4

110. Beaudoin-Bussières G, Chen Y, Ullah I, Prévost J, Tolbert WD, Symmes K, et al. An anti-SARS-CoV-2 non-neutralizing antibody with Fc-effector function defines a new NTD epitope and delays neuroinvasion and death in K18-hACE2 mice [Internet]. 2021 Sep [cited 2021 Nov 16] p. 2021.09.08.459408. Available from: https://www.biorxiv.org/content/10.1101/2021.09.08.459408v1

111. Plante JA, Liu Y, Liu J, Xia H, Johnson BA, Lokugamage KG, et al. Spike mutation D614G alters SARS-CoV-2 fitness. Nature. 2021 Apr;592(7852):116–21.

Appendix

SAMPLE ID	AUC WT	AUC Sub-lineage 1	AUC Sub-lineage 2	AUC Sub-lineage 3	Fold Change					
					Wild type vs Sub-lineage 1	Wild type vs Sub-lineage 2	Wild type vs Sub-lineage 3	Sub-lineage 1 vs Sub-lineage 2	Sub-lineage 1 vs Sub-lineage 3	Sub-lineage 2 vs Sub-lineage 3
CoVFU001	10365,5	7943	4840	1999	1,30	2,14	5,19	1,64	3,97	2,42
CoVFU002	58954	17746	12529	8544	3,32	4,71	6,90	1,42	2,08	1,47
CoVFU003	10732,5	5443	5118	2297	1,97	2,10	4,67	1,06	2,37	2,23
CoVFU004	17732,5	10500	11621	5719	1,69	1,53	3,10	0,90	1,84	2,03
CoVFU005	25987,5	18005	14756	9025	1,44	1,76	2,88	1,22	2,00	1,64
CoVFU006	16059,5	15268	10529	14842	1,05	1,53	1,08	1,45	1,03	0,71
CoVFU007	9481	11470	8282	10941	0,83	1,14	0,87	1,38	1,05	0,76
CoVFU008	10877	10827	10402	14943	1,00	1,05	0,73	1,04	0,72	0,70
CoVFU009	13984,5	10848	9977	16313	1,29	1,40	0,86	1,09	0,66	0,61
CoVFU010	12857	16692	9377	14644	0,77	1,37	0,88	1,78	1,14	0,64
CoVFU011	4199	4672	3715	3725	0,90	1,13	1,13	1,26	1,25	1,00
CoVFU012	6428,5	3924	1431	2333	1,64	4,49	2,76	2,74	1,68	0,61
CoVFU013	1346	1238	731,7	938,1	1,09	1,84	1,43	1,69	1,32	0,78
CoVFU014	1451	801,6	738,3	584,6	1,81	1,97	2,48	1,09	1,37	1,26
CoVFU015	2430,5	1233	1763	690,6	1,97	1,38	3,52	0,70	1,79	2,55
CoVFU016	8662,5	9926	4451	5142	0,87	1,95	1,68	2,23	1,93	0,87
CoVFU018	1799,3	2470	637,2	2124	0,73	2,82	0,85	3,88	1,16	0,30
CoVFU019	2159,95	3751	823,1	1308	0,58	2,62	1,65	4,56	2,87	0,63
CoVFU020	1093,55	777,5	452,4	945,3	1,41	2,42	1,16	1,72	0,82	0,48
CoVFU021	616	526,4	526,5	1377	1,17	1,17	0,45	1,00	0,38	0,38
CoVFU022	30402	1266	6483	3784	24,01	4,69	8,03	0,20	0,33	1,71
CoVFU023	29863	3311	6196	6990	9,02	4,82	4,27	0,53	0,47	0,89
CoVFU024	43819	12223	20824	27015	3,58	2,10	1,62	0,59	0,45	0,77
CoVFU026	15648,5	7372	9197	13166	2,12	1,70	1,19	0,80	0,56	0,70
CoVFU028	6796	3961	5549	7995	1,72	1,22	0,85	0,71	0,50	0,69
CoVFU029	11727,5	6659	6672	14380	1,76	1,76	0,82	1,00	0,46	0,46
CoVFU033	8742	6744	4795	9695	1,30	1,82	0,90	1,41	0,70	0,49
CoVFU034	2972,5	832,3	1652	4436	3,57	1,80	0,67	0,50	0,19	0,37
CoVFU035	3136	3599	545,2	1712	0,87	5,75	1,83	6,60	2,10	0,32
CoVFU037	11414,5	10047	8520	10295	1,14	1,34	1,11	1,18	0,98	0,83
CoVFU038	483,2	5004	867,7	4805	0,10	0,56	0,10	5,77	1,04	0,18
CoVFU039	136,15	52,4	141,3	394	2,60	0,96	0,35	0,37	0,13	0,36
CoVFU040	1377,5	86,1	3948	9609	16,00	0,35	0,14	0,02	0,01	0,41
CoVFU041	23101	3823	31635	38787	6,04	0,73	0,60	0,12	0,10	0,82
CoVFU043	24812	20333	40269	44285	1,22	0,62	0,56	0,50	0,46	0,91
CoVFU044	10950,5	6165	17401	23069	1,78	0,63	0,47	0,35	0,27	0,75
CoVFU045	4420,5	2704	8635	9776	1,63	0,51	0,45	0,31	0,28	0,88
CoVFU046	3633	830,8	5260	5901	4,37	0,69	0,62	0,16	0,14	0,89
CoVFU048	5088,5	2425	10114	9527	2,10	0,50	0,53	0,24	0,25	1,06
CoVFU049	8112	2255	13623	22073	3,60	0,60	0,37	0,17	0,10	0,62
CoVFU050	13087,5	2380	8445	14708	5,50	1,55	0,89	0,28	0,16	0,57
CoVFU051	6067	240,7	343,9	2036	25,21	17,64	2,98	0,70	0,12	0,17

>2.0 ↓ in binding
>2.0 ↑ in binding

Supplementary Figure 1: The change in binding between wild type and sub-lineage spike proteins. Data showing the change in binding for each sample as a result of the Sub-lineage mutations in the SARS-CoV-2 spike glycoprotein. The fold change in binding was determined and samples with a greater than two-fold increase

were highlighted in green while those with a greater than two-fold decrease were highlighted red.